

Bilayer Skyrmions in Chiral Magnets and Quantum Entanglement

by

Mohammad Walid AlMasri

A Dissertation Submitted to the
Graduate School of Sciences and Engineering
in Partial Fulfillment of the Requirements for
the Degree of

Doctor of Philosophy

in

Physics



**KOÇ
UNIVERSITY**

16 January , 2020

Bilayer Skyrmions in Chiral Magnets and Quantum Entanglement

Koç University

Graduate School of Sciences and Engineering

This is to certify that I have examined this copy of a doctoral dissertation by

Mohammad Walid AlMasri

and have found that it is complete and satisfactory in all respects,
and that any and all revisions required by the final
examining committee have been made.

Committee Members:

Prof. Dr. Tekin Dereli

Prof. Dr. Özgür E. Müstecaplıođlu

Prof. Dr. Alper Kiraz

Prof. Dr. Ekrem Aydiner

Assoc. Prof. Dr. Özgür Akarsu

Date: _____



To my family

ABSTRACT

The antiferromagnetic coupling and entanglement between skyrmion lattices in magnetic bilayer systems are studied in thesis. We first formulate the problem of large bilayer skyrmions using $\mathbb{CP}^1 \otimes \mathbb{CP}^1$ theory. We have considered bilayer skyrmions under the presence of Dzyaloshinskii-Moriya (DMI) and Zeeman interactions confined in a two-dimensional chiral magnet such as $\text{Fe}_{0.5}\text{Co}_{0.5}\text{Si}$. We parametrize the bilayer skyrmions using $SU(4)$ representation, and represent each skyrmion and antiskyrmion using Schmidt decomposition. Moreover, we computed the reduced density matrices for skyrmion and antiskyrmion. The conditions for maximal, partial entanglement and separable bilayer skyrmions are presented. We find intimate connection between bilayer skyrmions and $SU(4)$ skyrmions in multicomponent Hall systems and Graphene from entanglement perspective. Our results can be used for generating entanglement in systems with large number of spins.

ÖZETÇE

Bu tezde, çift-katmanlı manyetik sistemlerdeki Skyrmiyon örgülerinde komşu katmanlar arasındaki anti-ferromanyetik bağları ve kuantum dolanıklığını çalışmaktayız. Önce $\mathbb{CP}^1 \otimes \mathbb{CP}^1$ teorisini kullanarak büyük çift-katmanlı Skyrmiyon problemini tanımlamaktayız. Ele aldığımız $\text{Fe}_{0.5}\text{Co}_{0.5}\text{Si}$ gibi kiral miknatıslardaki çift-skyrmiyonlar arasında, 2-boyuta kısıtlanmış DM ve Zeeman etkileşmeleri bulunmaktadır. Çift-katmanlı Skyrmiyonların $SU(4)$ temsilini ele alarak her bir Skyrmiyon ve anti-Skyrmiyonu Schmidt ayrışımına göre temsil etmekteyiz. Bu tür çift-katmanlı Skyrmiyonların maksimal ve kısmen dolanıklığı ile ayrışıklığını belirleyen şartları vermekteyiz. Kuantum dolanıklığı yönünden ele alınca çok-bileşenli Hall sistemlerindeki veya grafendeki $SU(4)$ Skyrmiyonları ile çift-katmanlı Skyrmiyonlar arasında yakın bir ilişkinin kurulabildiği bu tezde gösterilmektedir. Bulgularımızın çok spinli dolanık sistemlerin oluşturulmasında yararlı olabileceğini düşünmekteyiz.

ACKNOWLEDGMENTS

I would like to warmly thank my supervisor Professor Tekin Dereli for all of his support, patience and guidance throughout my PhD studies. I am indebted to Prof. George Thompson and Prof. Kumar S.Narain who were my supervisors in the pre-PhD programme at International Center for Theoretical Physics (ICTP-Trieste).

I am grateful to Prof.Özgür E. Müstecaplıoğlu, Prof. Alper Kiraz, Prof. Ekrem Aydiner and Dr. Özgür Akarsu for being in my Ph.D. defense committee. I would like to express appreciation to ICTP director Prof. Fernando Quevedo for his support and encouragement.

Finally I would like to thank Koç University for Ph.D scholarship and all the support during my study period.

TABLE OF CONTENTS

List of Figures	ix
Nomenclature	xi
Chapter 1: Introduction	1
1.1 The history of skyrmions	1
1.2 Thesis Plan	3
1.3 Author's papers	3
Chapter 2: Topological Solitons	4
2.1 Kinks	4
2.2 Non-linear Sigma Models	7
2.3 Baby Skyrmions	9
2.4 Skyrmions	11
Chapter 3: Theoretical Aspects of Magnetic Skyrmions	12
3.1 Quantum Spin Dynamics and the Landau Lifshitz (LL)-Equation . .	13
3.2 The Spin Path Integral and Geometric Phase	14
3.3 Landau-Lifshitz-Gilbert Equation	19
3.4 Skyrmions in Chiral Magnets	20
3.4.1 Dzyaloshinskii-Moriya (DM) Interaction	20
3.4.2 Landau Theory	22
3.4.3 The Ginzburg-Landau (GL)- Theory	22
3.4.4 Derrick-Hobart Theorem	25
3.4.5 \mathbb{CP}^1 -Theory of a Skyrmion Crystal	26

3.5	Skyrmion Equation of Motion Using LL Equation	31
3.6	Skyrmion Equation of Motion using LLG Equation	32
3.7	Stress-Energy Tensor For Magnetic Skyrmions	34
3.8	Skyrmion Equation of Motion from Field-Theory Approach	37
3.9	LLG Equation and Spin-Transfer Torque (STT)	40
3.10	Thiele Equation	41
3.11	Poisson Bracket Method in Magnetic Skyrmions	43
3.11.1	Quantization Setups	43
3.11.2	Poisson Brackets in Planar Magnets	44
3.12	The Interfacial DMI and Skyrmions in Thin Films	47
Chapter 4:	Quantum Entanglement	50
4.1	Qubits and Bloch Sphere	50
4.2	Density Operators	50
4.3	Schmidt Decomposition	52
4.4	Quantum Entanglement	52
4.5	Entanglement Entropy	53
Chapter 5:	$SU(4)$ description of bilayer skyrmion-antiskyrmion pairs	55
5.1	Motivation	55
5.2	The $\mathbb{CP}^1 \otimes \mathbb{CP}^1$ -Theory of Large Bilayer Skyrmion	56
5.3	$SU(4)$ Parametrization of Bilayer Skyrmion	61
5.4	Geometry of Bilayer Skyrmion	65
Chapter 6:	Conclusion	69
A	The Topological Charge Q_S	71
B	$SU(4)$ Representation	71
Bibliography		73

LIST OF FIGURES

2.1	Plot of $\tanh(x)$ with respect to the variable x in the interval $[-100, 100]$. Here we chosen $\lambda = 1$	6
2.2	Plot of $\theta(x) = \tan^{-1}[\exp(mx)]$ when $m = 1$ in the interval $[-10, 10]$, a solution of this type is usually referred to as "Kink".	8
2.3	Plot of $\theta(x) = \tan^{-1}[\exp(mx)]$ when $m = -1$ in the interval $[-10, 10]$, a solution of this type is usually referred to as "anti-Kink".	8
2.4	The spin configuration of baby skyrmion.	10
3.1	(a) Bloch (Vortex) skyrmion . (b) Néel (Hedgehog) skyrmion	12
3.2	The unit sphere \mathbb{S}^2 and the unit vectors \mathbf{n}_0 and \mathbf{n}	15
3.3	The DMI between spins \mathbf{S}_1 and \mathbf{S}_2 with DM constant D perpendicular to the line joining the two spins.	21
3.4	(a) MnSi structure as an example of B20 noncentrosymmetric crystal structures. (b) The Bloch- skyrmion configuration in MnSi.	25
3.5	Phase diagrams of magnetic structure and spin textures in a thin film of Fe _{0.5} Co _{0.5} Si in the B - T plane. H, SkX and FM denote the helical, skyrmion lattice and ferromagnetic phases respectively. B_C is the critical magnetic field for each phase, above this value the corresponding phase undergoes phase transition to the next phase in the chain H→ SkX → FM. Retrieved from [35]	30
4.1	Qubit representation on Bloch sphere.	51

5.1	The setup used in our study consists of two identical thin films fabricated from chiral magnets (CM1,CM2) separated by an insulating material (I). The insulating material is responsible for the antiferromagnetic coupling between spins in each ferromagnetic layer. Each chiral magnet supports the emergence of large Skyrmion phase under some specific conditions of magnetic field B and temperature T	59
5.2	The vector field plot of emergent gauge field \mathbf{a} . We found this figure to be the same for both skyrmion and its AFM-coupled antiskyrmion. In other words, large skyrmions and its AFM coupled antiskyrmions feel the same amount of fluxes.	61
5.3	plot of entanglement measure Ξ versus angle α and small angle variation $\delta = 0 \rightarrow 0.35$ radians . Maximal entanglement happens around $\frac{\pi}{2} + n\pi$. We observe that maximally entanglement measure is robust against small angle variations.	64
5.4	Bloch sphere representation of spin states $ \Phi_S\rangle = 0\rangle = (1\ 0)^T$, $ \Phi_A\rangle = 1\rangle = (0\ 1)^T$ and $ \Psi\rangle = (0\ \frac{1}{\sqrt{2}}\ \frac{1}{\sqrt{2}}\ 0)^T$	65

NOMENCLATURE



Chapter 1

INTRODUCTION

Since its first experimental observation in 2009 [1], magnetic skyrmions have been actively investigated in a wide range of materials such as bulk chiral magnets, ferromagnetic / heavy metal interfaces, insulating materials, antiferromagnetic materials, frustrated magnets and compensated ferrimagnets [2] - [13].

Magnetic skyrmions are topologically protected objects in the sense no continuous deformation can delete a skyrmion. This fact paved the way for considering isolated nanoscale magnetic skyrmions as information carriers in future spintronic devices [12, 14].

Skyrmion textures were first identified as mean field ground state configurations for models of anisotropic noncentrosymmetric magnetic materials with chiral spin-orbit interactions subjected to an external magnetic field [2, 3].

1.1 *The history of skyrmions*

Skyrmions were introduced by T.Skyrme [15] as a nonlinear field theory of pions in three spatial dimensions. Although not involving quarks, it can be regarded as an approximate, low effective theory of QCD, becoming exact as the number of quark colours becomes large. Let us denote the Skyrme field by $U(t, \mathbf{x})$, being an $SU(2)$ -valued scalar field, the Skyrme model has the Lagrangian

$$L = \int d^3x \left\{ \frac{F_\pi^2}{16} \text{Tr}(\partial_\mu U \partial^\mu U) + \frac{1}{32e^2} \text{Tr}([\partial_\mu U U, \partial_\nu U U][\partial^\mu U U, \partial^\nu U U]) \right\}, \quad (1.1)$$

Here F_π and e are fixed parameters. By scaling the Lagrangian in units of $F_\pi/4e$ and length in units of $2/eF_\pi$, the standard Skyrme Lagrangian takes the simple form

$$L = \int d^3x \left\{ -\frac{1}{2} \text{Tr}(R_\mu R^\mu) + \frac{1}{16} \text{Tr}([R_\mu, R_\nu][R^\mu, R^\nu]) \right\}, \quad (1.2)$$

where we have introduced the $SU(2)$ -valued current $R_\mu = (\partial_\mu U) U$. The Euler-Lagrange equation which results from the Skyrme Lagrangian is

$$\partial_\mu (R^\mu + \frac{1}{4} [R^\nu, [R_\nu, R^\mu]]) = \partial_\mu \tilde{R}^\mu = 0 \quad (1.3)$$

The Skyrme field equation is a nonlinear wave equation for $U(t, \mathbf{x})$ configuration. It takes the form of continuity equation by defining $\tilde{R}_\mu := (R^\mu + \frac{1}{4} [R^\nu, [R_\nu, R^\mu]])$. We impose the following boundary conditions for the field configuration $U(t, \mathbf{x}) \rightarrow \mathbb{I}_2$ as $\mathbf{x} \rightarrow \infty$ for all \mathbf{x} . From this constraint, we realize that position space \mathbb{R}^3 can be compactified to the surface \mathbb{S}^3 of a three-dimensional sphere.

The Skyrme Lagrangian has an $\frac{SU(2) \otimes SU(2)}{\mathbb{Z}_2} \cong SO(4)$ chiral symmetry corresponding to the transformation $U \rightarrow \mathcal{O}_1 U \mathcal{O}_2$, where \mathcal{O}_1 and \mathcal{O}_2 are constant elements of $SU(2)$. The boundary condition $U(\infty) \rightarrow \mathbb{I}_2$ spontaneously breaks this chiral symmetry to an $SO(3)$ isospin symmetry given by conjugation

$$U \rightarrow \mathcal{O} U \mathcal{O}^\dagger, \quad (1.4)$$

where $\mathcal{O} \in SU(2)$. The matrix $U(t, \mathbf{x})$ can be parametrized as

$$U(t, \mathbf{x}) = \begin{pmatrix} \phi_1(t, \mathbf{x}) + i\phi_2(t, \mathbf{x}) & \phi_3(t, \mathbf{x}) - i\phi_4(t, \mathbf{x}) \\ -\phi_3(t, \mathbf{x}) + i\phi_4(t, \mathbf{x}) & \phi_1(t, \mathbf{x}) - i\phi_2(t, \mathbf{x}) \end{pmatrix} \quad (1.5)$$

The real fields ϕ_α , $\alpha = 1 \dots 4$ satisfy the constraint

$$\phi_1^2 + \phi_2^2 + \phi_3^2 + \phi_4^2 = 1. \quad (1.6)$$

Thus for a fixed time t , the field $\phi \equiv (\phi_1, \phi_2, \phi_3, \phi_4)$ defines a mapping from \mathbb{S}^3 to \mathbb{S}^3 . In homotopy theory, this situation corresponds to $\pi_3(\mathbb{S}^3) = \mathbb{Z}$. The field configuration at any time can be labeled by an integer winding number

$$W = \frac{1}{2\pi^2} \int d^3x \varepsilon_{ijkl} \frac{\partial \phi_j}{\partial x_1} \frac{\partial \phi_k}{\partial x_2} \frac{\partial \phi_l}{\partial x_3}, \quad (1.7)$$

where $\mathbf{x} = (x_1, x_2, x_3)$ and ε_{ijkl} is the totally antisymmetric tensor.

1.2 Thesis Plan

In chapter 2, we present a general introduction to topological solitons.

In chapter 3, we theoretically study magnetic skyrmions in detail.

In chapter 4, we provide some basic definitions related to quantum entanglement.

The novel results in this thesis are presented in chapter 5 where I have studied bilayer skyrmions in a system of two perpendicular chiral thin films with insulating spacer between them. In this thesis, We study quantum entanglement in bilayer skyrmions (skyrmion-antiskyrmion pairs) from a geometrical point of view.

At the end we summarizes the novel results in the conclusion which makes the chapter 6. Thesis is followed by two appendices about topological charge of magnetic skyrmion and $SU(4)$ representations.

1.3 Author's papers

During the course of my Ph.D. studies I have produced the following papers

- M.W.AlMasri, “ $SU(4)$ description of bilayer skyrmion-antiskyrmion pairs”, to appear in Europhysics Letters 2020, <https://arxiv.org/abs/1909.10483>.
- M.W.AlMasri, “ Axial-anomaly in noncommutative QED and Pauli–Villars regularization” International Journal of Modern Physics A: Vol.34, No.26, 1950150 (2019).

Chapter 2

TOPOLOGICAL SOLITONS

Some specific stable solutions of classical nonlinear equations support extended objects known as solitons.

In quantum field theory, solitons are coherent states describing collective excitations of the basic field. Solitons are topological objects if and only if their stability is assured topologically. Examples are skyrmions, vortices and kinks [17]. In this chapter, we will give an overview of topological solitons that will help understand basic features of skyrmions.

2.1 *Kinks*

Solitons are classical solutions of non-linear equations which are non-singular with finite energy, and localized in space. Topological Solitons are solitons which can not be deformed continuously to the vacuum.

Consider a pair of real-valued fields $\mathbf{n} = (n_1, n_2)$ that are functions of time t and one spatial coordinate x . A simple Lagrangian that is symmetric under rotation $\mathbf{n} \rightarrow \mathcal{R}\mathbf{n}$, where \mathcal{R} being an element of $O(2)$ Lie group is

$$L = \frac{1}{2} \int dx [(\partial_t \mathbf{n})^2 - (\partial_x \mathbf{n})^2 - m^2 \mathbf{n} \cdot \mathbf{n}], \quad (2.1)$$

The associated Euler-Lagrange equation is a linear differential equation known as Klein-Gordon equation

$$(-\partial_t^2 + \partial_x^2 - m^2) \mathbf{n} = 0 \quad (2.2)$$

The above model is an example of a linear field theory. Basically, to make it a nonlinear field theory, one can either add higher-order terms of \mathbf{n} and its derivatives

or imposing a constraints on the fields \mathbf{n} itself. In this chapter, we will follow the second approach developed by Tony Skyrme in the late 50s. One way to impose a constraint on the field in Lagrangian 2.1 is by treating \mathbf{n} as a point on unit circle \mathbb{S}^1 . Mathematically, this constraint reads as

$$\mathbf{n} \cdot \mathbf{n} = n_1^2 + n_2^2 = 1. \quad (2.3)$$

We can parametrize the field \mathbf{n} in terms of angle θ in a way that take cares of the constraint 2.3,

$$\mathbf{n} = (\cos \theta, \sin \theta). \quad (2.4)$$

Under this parametrization, the Lagrangian 2.1 becomes

$$L = \frac{1}{2} \int dx [(\partial_t \theta)^2 - (\partial_x \theta)^2 - m^2] \quad (2.5)$$

Remarkably, the mass term becomes a constant due to the imposed constraint. It is safe to remove the mass term in the above Lagrangian since it will have no effect on equations of motion. The corresponding conserved currents related to the Lagrangian 2.5 are given by

$$J_\alpha = \frac{1}{2\pi} \varepsilon_{\alpha\beta} \varepsilon_{ab} n_a \partial_\beta n_b. \quad (2.6)$$

The first of the two antisymmetric tensors, $\varepsilon_{\alpha\beta}$ denotes the spacetime index (t, x) , while the second ε_{ab} denotes the index of field component $\mathbf{n} = (n_1, n_2)$. The above topological current has two components (J_t, J_x) defined as

$$\begin{aligned} J_t &= \frac{1}{2\pi} \partial_x \theta, \\ J_x &= -\frac{1}{2\pi} \partial_t \theta. \end{aligned} \quad (2.7)$$

The above current components obey the continuity equation $\partial_t J_t + \partial_x J_x = 0$. Here J_t plays the role of “charge” and J_x plays the role of “current density”. The total charge is given by

$$Q(t) = \int_{-\infty}^{\infty} \rho(x, t) dx = \frac{1}{2\pi} \int_{-\infty}^{\infty} \partial_x \theta(x, t) dx = \frac{1}{2\pi} [\theta(\infty, t) - \theta(-\infty, t)]. \quad (2.8)$$

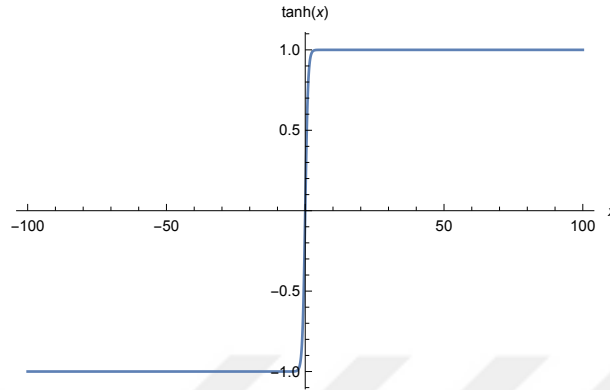


Figure 2.1: Plot of $\tanh(x)$ with respect to the variable x in the interval $[-100, 100]$. Here we chosen $\lambda = 1$.

We apply the periodic boundary condition $\theta(\infty, t) = \theta(-\infty, t) + 2\pi N$, where N is an integer number. The charge becomes $Q(t) = N$ as expected.

Consider a simple field configuration localized in space and carrying a nonzero charge $Q = 1$ defined as

$$\theta(x) = \pi \tanh\left(\frac{x}{\lambda}\right) \quad (2.9)$$

This field varies from $-\pi$ at $-\infty$ to π at ∞ regardless of the value for λ . However, the sign of λ can affect the above assumptions. The energy of the soliton with θ configuration is given by

$$H = \frac{1}{2} \int (\partial_x \theta)^2 dx = \frac{\pi^2}{2\lambda^2} \int [\coth(\frac{x}{\lambda})]^2 dx = \frac{\pi^2}{2\lambda} \int (\coth y)^2 dy. \quad (2.10)$$

Here $y = \frac{x}{\lambda}$. As seen from 2.10, the energy of the solitons decreases when the parameter λ increases, the most energetically stable configuration is when $\lambda = \infty$. Thus, the above soliton enjoys topological protection but not energetically stable that would preserve its locality in space.

To guarantee that a given nontrivial soliton configuration remains energetically stable as well as topologically protected, we need to add extra terms to the Lagrangian

2.1. The new term is invariant under reflection $\mathbf{n} \rightarrow -\mathbf{n}$ and rotation by $\frac{\pi}{2}$. The lowest-order term satisfying these conditions is the fourth-power term: $\mathbf{n}^4 = n_1^4 + n_2^4$. With this new term, the Lagrangian reads

$$\begin{aligned} L &= \frac{1}{2} \int dx [(\partial_t \mathbf{n})^2 - (\partial_x \mathbf{n})^2 - \frac{1}{8} m^2 (n_1^4 + n_2^4)] \\ &= \frac{1}{2} \int dx [(\partial_t \theta)^2 - (\partial_x \theta)^2 - \frac{1}{8} m^2 (1 - \cos 4\theta)]. \end{aligned} \quad (2.11)$$

With the new interaction term, the Euler-Lagrange equation reads

$$\partial_t^2 \theta - \partial_x^2 \theta + \frac{1}{4} m^4 \sin 4\theta = 0. \quad (2.12)$$

Which is known as sine-Gordon equation. It considers as one of the basic examples in nonlinear field theory with a known exact solution. In small angle limit, $\sin \theta \approx \theta$, it reduces to Klein-Gordon equation. In the static limit when $\theta(t, x) = \theta(x)$, the sine-Gordon equation becomes

$$-\partial_x^2 \theta + \frac{1}{4} m^2 \sin 4\theta = 0. \quad (2.13)$$

So that its solution is given by

$$\theta(x) = \tan^{-1}[\exp(mx)]. \quad (2.14)$$

When $m > 0$, θ evolves from 0 to $\frac{\pi}{2}$ as quarter-charged Soliton. When $m < 0$, θ evolves from $\frac{\pi}{2}$ to 0 as an anti-Soliton with quarter topological charge. The one-dimensional topological Solitons are usually called Kinks for positive Q and anti-Kinks for negative Q . We plotted the Kink and anti-Kink in 2.1 and 2.1. The nature of kink solution is such that it connects one minimum of the potential $V(\theta) = (1 - \cos 4\theta)$ to another.

2.2 Non-linear Sigma Models

A non-linear sigma model (NL σ M) is a scalar field theory whose scalar fields defines a map from space-time to a Riemannian target manifold. The $O(n)$ NL σ M is defined by the action

$$S[\mathbf{n}] = \frac{1}{2\lambda^2} \int d^d x \partial^\mu \mathbf{n} \cdot \partial_\mu \mathbf{n}, \quad (2.15)$$

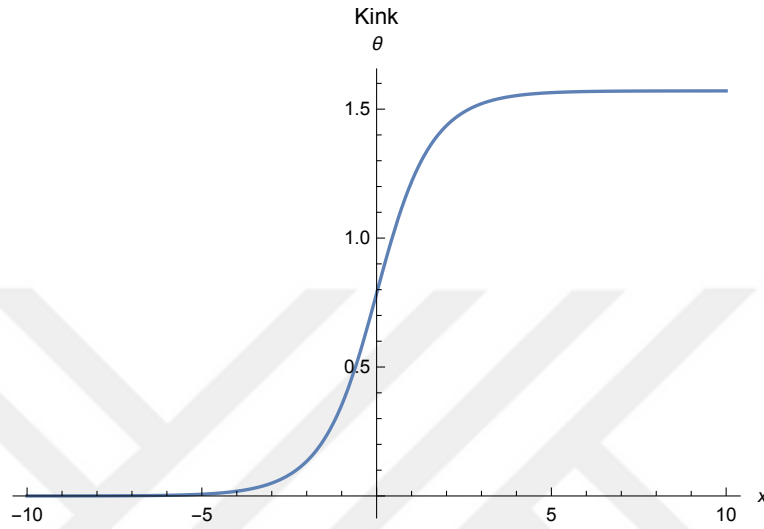


Figure 2.2: Plot of $\theta(x) = \tan^{-1}[\exp(mx)]$ when $m = 1$ in the interval $[-10,10]$, a solution of this type is usually referred to as "Kink".

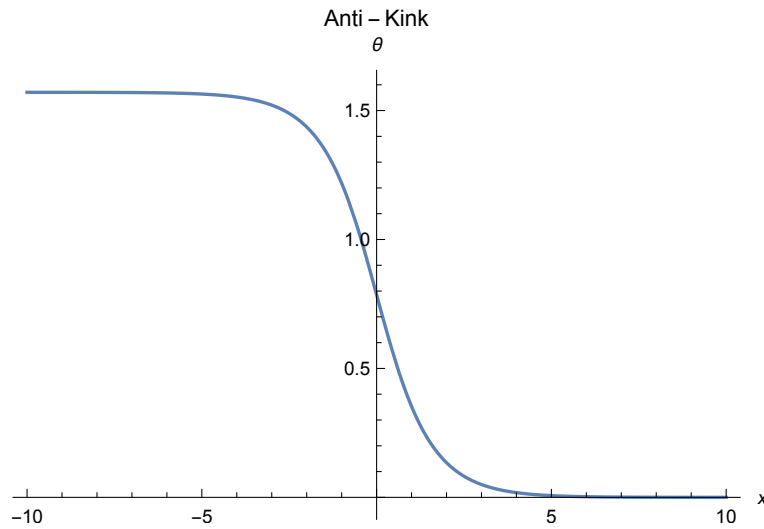


Figure 2.3: Plot of $\theta(x) = \tan^{-1}[\exp(mx)]$ when $m = -1$ in the interval $[-10,10]$, a solution of this type is usually referred to as "anti-Kink".

where the real scalar fields $\mathbf{n}(x^\mu)$ obey the constraint $\mathbf{n} \cdot \mathbf{n} = \text{constant}$. We adopted the Einstein summation notation for repeated indices $\partial_\mu \mathbf{n} \cdot \partial_\mu \mathbf{n} \equiv \Sigma_\mu \partial_\mu \mathbf{n} \cdot \partial_\mu \mathbf{n}$, where μ denotes spacetime coordinates. One interesting case is the $O(3)$ nonlinear σ model in (1+1)dimensions, where $\mathbf{n} = (n_1, n_2, n_3)$ and $\mathbf{n} \cdot \mathbf{n} = 1$. In statistical physics, $O(3)$ nonlinear σ model is realized the continuum limit of an isotropic ferromagnet [18]. Throughout the current thesis, we shall use this model extensively during our study of baby skyrmions in (2+1) dimensions.

2.3 Baby Skyrmions

Baby skyrmions are topological solitons in 2 + 1- dimensions of a certain class of non-linear sigma models. The associated topological current density vector is given by

$$J_\alpha = \frac{1}{8\pi} \varepsilon_{\alpha\beta\gamma} \varepsilon_{abc} n_a \partial_\beta n_b \partial_\gamma n_c. \quad (2.16)$$

The conserved charge is given by integrating over the temporal-component of J_α

$$\begin{aligned} Q_S &= \frac{1}{8\pi} \int dx dy \varepsilon_{abc} n_a (\partial_x n_b \partial_y n_c - \partial_y n_b \partial_x n_c) \\ &= \frac{1}{4\pi} \int dx dy \mathbf{n} \cdot \left(\frac{\partial \mathbf{n}}{\partial x} \times \frac{\partial \mathbf{n}}{\partial y} \right). \end{aligned} \quad (2.17)$$

The topological charge Q counts how many times $\mathbf{n}(\mathbf{r}) = \mathbf{n}(x, y)$ wraps the unit sphere. Baby skyrmion profile \mathbf{n} is of the form

$$\mathbf{n} = (\sin[f(r)] \cos[N\phi], \sin[f(r)] \sin[N\phi], \cos[f(r)]), \quad (2.18)$$

where f is a radial function that depends on r and N is an integer. The relation 2.18 reduces to the spherical unit vector by sending $f(r) \rightarrow r$ and setting $N = 1$. Feeding 2.18 in 2.17 gives the skyrmion charge,

$$Q_S = \frac{N}{2} \int_0^\infty dr f(r)' \sin[f(r)] = \frac{N}{2} \int_0^\infty dr \frac{dn^z}{dr} = N \cdot \frac{n^z(0) - n^z(\infty)}{2} = \pm N. \quad (2.19)$$

The charge density ρ_S is

$$\rho_S(x, y) = \frac{1}{4\pi} \mathbf{n} \cdot (\partial_x \mathbf{n} \times \partial_y \mathbf{n}) = \frac{N}{4\pi r} f'(r) \sin[f(r)]. \quad (2.20)$$

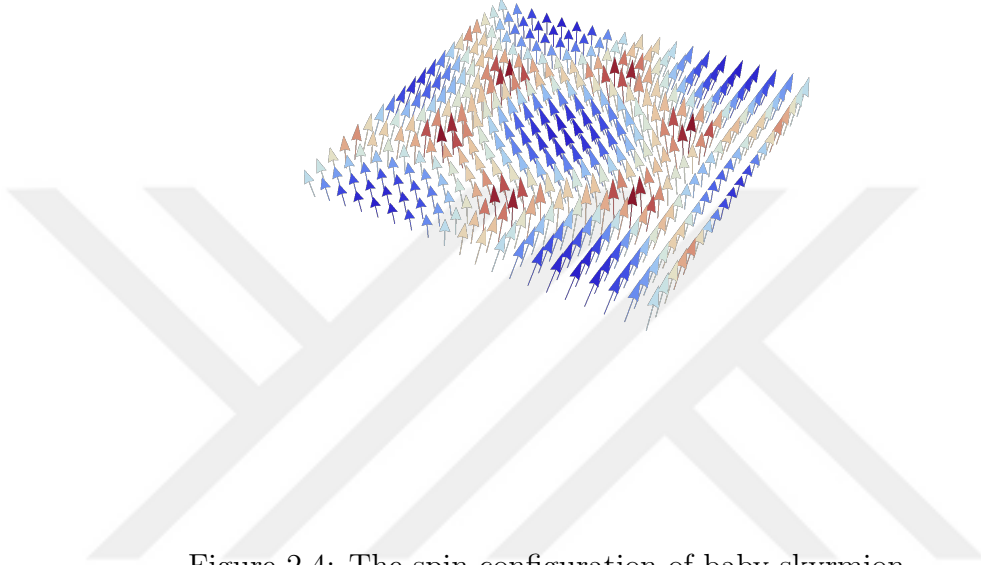


Figure 2.4: The spin configuration of baby skyrmion.

The baby Skyrmion Hamiltonian is

$$H = \frac{1}{2} \int dx dy [(\partial_x \mathbf{n})^2 + (\partial_y \mathbf{n})^2]. \quad (2.21)$$

Its associated energy is found by plugging 2.18 in 2.21,

$$E_S = \pi \int_0^\infty r dr [(f')^2 + \frac{N^2}{r^2} (\sin f)^2]. \quad (2.22)$$

The saddle-point equation following from the baby skyrmion energy functional is

$$2(r f')' + \frac{N^2}{r^2} \sin^2 f = 0. \quad (2.23)$$

In chiral magnets, the Hamiltonian 2.21 can not stabilize skyrmion by itself, it requires extra terms such as Dzyaloshinskii-Moriya (DM) and Zeeman interactions. In this thesis, our main interest is baby skyrmions only. Magnetic skyrmion throughout the present thesis is the same as baby skyrmion described in this section plus some extra interaction terms.

2.4 Skyrmions

Skyrmions are topological solitons in 3+1-dimensions with certain field configurations.

The topological current for skyrmion is given by

$$J_\alpha = \frac{1}{12\pi^2} \varepsilon_{\alpha\beta\gamma\delta} \varepsilon_{abcd} n_a \partial_\beta n_b \partial_\gamma n_c \partial_\delta n_d. \quad (2.24)$$

Where $\mathbf{n} = (n_1, n_2, n_3, n_4)$ is a four-component field with constraint $\mathbf{n} \cdot \mathbf{n} = 1$. The skyrmion profile is

$$\mathbf{n} = \left(\sin[f(r)] \frac{x}{r}, \sin[f(r)] \frac{y}{r}, \sin[f(r)] \frac{z}{r}, \cos[f(r)] \right). \quad (2.25)$$

The temporal component of the topological current J_α gives the charge density, that is

$$\rho_S(r) = \frac{1}{2\pi^2} \frac{(\sin[f])^2 f'}{r^2}, \quad (2.26)$$

Its integral over the whole space gives the associated topological charge,

$$\begin{aligned} Q_S &= 4\pi \int_0^\infty \rho_S(r) r^2 dr = \frac{2}{\pi} \int_{f(\infty)}^{f(0)} (\sin[f])^2 df = \frac{1}{\pi} \int_{f(\infty)}^{f(0)} (1 - \cos[2f]) df \quad (2.27) \\ &= \frac{f(0) - f(\infty)}{\pi} - \frac{\sin[2f(0)] - \sin[2f(\infty)]}{2\pi} = \frac{f(0) - f(\infty)}{\pi}. \end{aligned}$$

Where the boundary conditions for the radial function $f(r)$ are $f(0) = \pi + 2n\pi$ and $f(\infty) = 2n\pi$, $n = 0, 1, 2, \dots$. This explains why $\sin[2f(0)] - \sin[2f(\infty)] = 0$. Thus, the quantity $\frac{f(0)-f(\infty)}{\pi}$ is an integer number as expected.

Chapter 3

THEORETICAL ASPECTS OF MAGNETIC SKYRMIONS

Magnetic Skyrmions are microscopic topological defects in spin textures characterized by the topological winding or skyrmion number Q_S

$$Q_S = \frac{1}{4\pi} \int d^2\mathbf{r} \mathbf{n} \cdot \left(\frac{\partial \mathbf{n}}{\partial x} \times \frac{\partial \mathbf{n}}{\partial y} \right). \quad (3.1)$$

In mathematics, Q_S is called the Pontryagin number. It counts how many times $\mathbf{n}(\mathbf{r}) = \mathbf{n}(x, y)$ wraps the unit sphere [16, 17].

Skyrmions were first introduced by Tony Skyrme [15] to explain hadrons in nuclei. Interestingly it has also turned out to be relevant in condensed matter systems such as chiral magnets [1], Bose-Einstein condensates [19], liquid crystals [20], quantum Hall effects [21, 22] and many others...

There are two distinct types of magnetic skyrmions : the Néel-type and Bloch-type. These correspond to different directions of the rotation as shown in the figure 3.

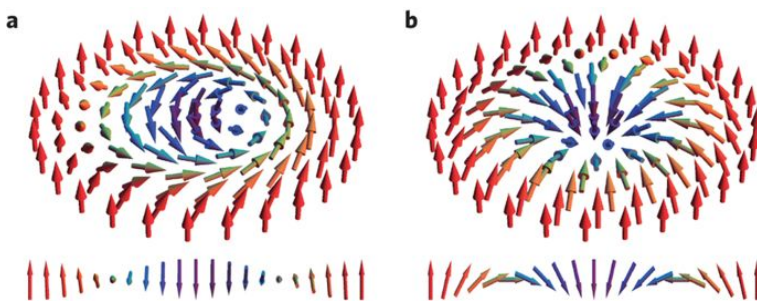


Figure 3.1: (a) Bloch (Vortex) skyrmion . (b) Néel (Hedgehog) skyrmion

In most cases, the chiral interactions between atomic spins in non-centrosymmetric

magnetic compounds (B20 crystal structure) induce skyrmions in magnetic materials [4, 5].

3.1 Quantum Spin Dynamics and the Landau Lifshitz (LL)-Equation

Since our interest is in magnetic moments of localized electrons whose spins are free to rotate, we consider the simplest model which exhibits the spin dynamics is the Zeeman Hamiltonian which describes the electron with mass m_e and charge e under presence of an external magnetic field \mathbf{B}

$$H_Z = \frac{e\hbar}{2m_e} \boldsymbol{\sigma} \cdot \mathbf{B} = \mu_B \boldsymbol{\sigma} \cdot \mathbf{B}, \quad (3.2)$$

where μ_B is the Bohr magneton and $\boldsymbol{\sigma} = (\sigma_x, \sigma_y, \sigma_z)$ is the Pauli vector.

We derive the equation of motion for electron's spin operator using the Heisenberg representation. The time evolution of any operator $\mathcal{O}(t) = e^{i\frac{Ht}{\hbar}} \mathcal{O} e^{-i\frac{Ht}{\hbar}}$ follows directly from its commutator with the Hamiltonian $\dot{\mathcal{O}}(t) = \frac{i}{\hbar}[H, \mathcal{O}(t)]$. Applying this rule in the Zeeman Hamiltonian alongside with the commutation algebra of spin operators $[S_\alpha, S_\beta] = i\hbar \varepsilon_{\alpha\beta\gamma} S_\gamma$ gives the simplest first-order differential equation for the spin precession

$$\dot{\mathbf{S}} = \mathbf{S} \times \left(-\frac{\delta H_z}{\delta \mathbf{S}}\right). \quad (3.3)$$

Since in an experiment one measures the magnetic moment, not the spin itself, it is more convenient to write the equation 3.3 in terms of the magnetic moment $\vec{\mu}$.

The relation between $\vec{\mu}$ and spin \mathbf{S} is linear as

$$\vec{\mu} = -\frac{ge}{2m} \mathbf{S} = -\gamma \mathbf{S}, \quad (3.4)$$

where g denotes Lande g-factor which is approximately equal to 2 for electrons, γ is the gyromagnetic ratio and defined as a positive quantity. One can consider μ as a classical vector of length M and write $\mu = M\mathbf{n}$ where \mathbf{n} is an arbitrary unit vector. Replacing \mathbf{S} by $-\frac{M\mathbf{n}}{\gamma}$ in 3.3 gives

$$\dot{\mathbf{n}} = \frac{\gamma}{M} \mathbf{n} \times \frac{\delta H_Z}{\delta \mathbf{n}}. \quad (3.5)$$

Interestingly, the previous equation 3.5 can be generalized easily to any spin Hamiltonian by replacing $\frac{\delta H_Z}{\delta \mathbf{S}}$ with the variational derivative $\frac{\delta H}{\delta \mathbf{S}}$.

The semi-classical equation above for spin dynamics is known as the Landau-Lifshitz (LL) equation. This formula was proposed in 1935 by Lev Landau and Evgeny Lifshitz [23]. Since most of our studies will be for negatively charged particles, namely the electrons, the substitution \mathbf{n} with $-\mathbf{n}$ in the equation 3.5 is legitimate. This means that spin of electron will be in the opposite direction to the magnetization. Therefore, LL equation takes the form

$$\dot{\mathbf{n}} = -\frac{\gamma}{M} \mathbf{n} \times \frac{\delta H}{\delta \mathbf{n}}. \quad (3.6)$$

We can define the force vector as $\mathbf{h}_{eff} = -\frac{\delta H}{\delta \mathbf{n}}$ and express the LL equation in the form

$$\dot{\mathbf{n}} = \frac{\gamma}{M} \mathbf{n} \times \mathbf{h}_{eff}. \quad (3.7)$$

3.2 The Spin Path Integral and Geometric Phase

Consider a spin- S degree of freedom coupled to an external field through a Zeeman-like interaction term. From standard quantum mechanics we know that Zeeman term breaks down the $(2S + 1)$ -fold degeneracy. This will result in $(2S + 1)$ non-degenerate energy levels. The path integral formalism will allow us to study the evolution operator between arbitrary initial and final states.

Let us begin by describing the Hilbert space in a simple manner. We have $2S + 1$ states that transform like a spin- S representation of $SU(2)$. Let $|0\rangle$ denote the highest-weight state in this representation [24]

$$|0\rangle = |S, S\rangle. \quad (3.8)$$

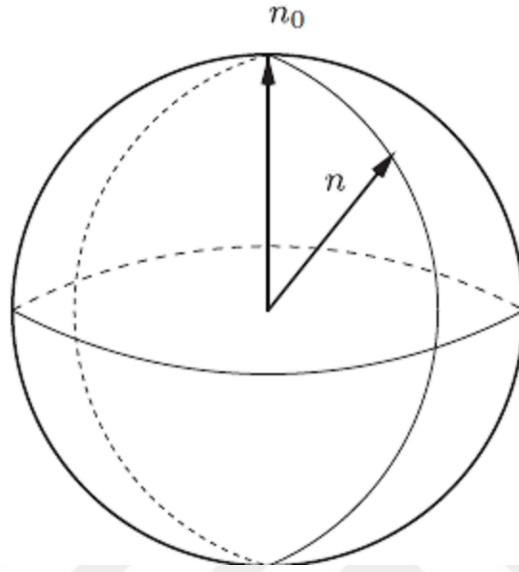


Figure 3.2: The unit sphere \mathbb{S}^2 and the unit vectors \mathbf{n}_0 and \mathbf{n} .

This state is an eigenstate both of S_z , the only diagonal generator of $SU(2)$, and the quadratic Casimir invariant \mathbf{S}^2 :

$$\begin{aligned} S_z |0\rangle &= S |0\rangle, \\ \mathbf{S}^2 |0\rangle &= S(S+1) |0\rangle. \end{aligned} \tag{3.9}$$

Now consider the state $|\mathbf{n}\rangle$ labeled by the unit vector \mathbf{n} which is obtained by the rotation

$$|\mathbf{n}\rangle = e^{i\theta(\mathbf{n}_0 \times \mathbf{n}) \cdot \mathbf{S}} |S, S\rangle. \tag{3.10}$$

Where \mathbf{n}_0 is a unit vector along the quantization axis, θ is the co-latitude such that $\mathbf{n}_0 \cdot \mathbf{n} = \cos \theta$ (see figure 3.2) and S_i ($i = x, y, z$) are the three generators of $SU(2)$ in the spin- S representation.

The state $|\mathbf{n}\rangle$ could be expanded in a complete basis of the spin- S irreducible representation $\{|S, m\rangle\}$, where m labels the eigenvalues of diagonal element S_z ,

$$\begin{aligned} S_z |S, m\rangle &= m |S, m\rangle, \\ \mathbf{S}^2 |S, m\rangle &= S(S+1) |S, m\rangle. \end{aligned} \tag{3.11}$$

and $-S \leq m \leq S$, in integer steps. The coefficients of expansion are the representation matrices $D^{(S)}(\mathbf{n})_{mS}$ such that

$$|\mathbf{n}\rangle = \sum_{m=-S}^S D^{(S)}(\mathbf{n})_{mS} |S, m\rangle. \quad (3.12)$$

The matrices D_{Sm}^S do not form a group but rather obey the algebra

$$D^{(S)}(\mathbf{n}_1)_{mS} D^{(S)}(\mathbf{n}_2)_{mS} = D^{(S)}(\mathbf{n}_3)_{mS} e^{i\Phi(\mathbf{n}_1, \mathbf{n}_2, \mathbf{n}_3)} \quad (3.13)$$

\mathbf{n}_1 , \mathbf{n}_2 , and \mathbf{n}_3 are three arbitrary unit vectors on the unit sphere \mathbb{S}^2 and $\Phi(\mathbf{n}_1, \mathbf{n}_2, \mathbf{n}_3)$ is the area of the spherical triangle with vertices at \mathbf{n}_1 , \mathbf{n}_2 , and \mathbf{n}_3 .

The inner product of the spin coherent states $|\mathbf{n}_1\rangle$ and $|\mathbf{n}_2\rangle$ is given by

$$\langle \mathbf{n}_1 | \mathbf{n}_2 \rangle = \langle 0 | D^{(S)\dagger}(\mathbf{n}_1) D^{(S)}(\mathbf{n}_2) | 0 \rangle = e^{i\Phi(\mathbf{n}_1, \mathbf{n}_2, \mathbf{n}_0)} \left(\frac{1 + \mathbf{n}_1 \cdot \mathbf{n}_2}{2} \right)^S. \quad (3.14)$$

The diagonal matrix elements of the $SU(2)$ generators of \mathbf{S}

$$\langle \mathbf{n} | \mathbf{S} | \mathbf{n} \rangle = S \mathbf{n}. \quad (3.15)$$

and the identity operator in terms of spin coherent state $|\mathbf{n}\rangle$ is

$$\hat{I} = \frac{2S+1}{4\pi} \int d^3\mathbf{n} \delta(\mathbf{n}^2 - 1) |\mathbf{n}\rangle \langle \mathbf{n}|. \quad (3.16)$$

Let $H = \mathbf{B} \cdot \mathbf{S}$ be the Zeeman-like Hamiltonian with one spin- S degree of freedom.

We shall write the evolution operator in imaginary time as

$$Z = \text{Tr} e^{iHT} = \text{Tr} e^{-\beta H} \quad (3.17)$$

Here we assume the initial and final states being identified precisely. Let us divide the imaginary-time interval into N_t steps each of length δt and consider the limit $N_t \rightarrow \infty$ and $\delta t \rightarrow 0$ while keeping their product constant equal to β . It is customary to make use of the Trotter formula

$$Z = \text{Tr} e^{-\beta H} = \lim_{\substack{\delta t \rightarrow 0 \\ N_t \rightarrow \infty}} (e^{-\delta t H})^{N_t} \quad (3.18)$$

and insert the identity operator 3.16 in the relation 3.17 at every step t_i . We obtain

$$Z = \lim_{\substack{\delta t \rightarrow 0 \\ N_t \rightarrow \infty}} \left(\prod_{i=1}^{N_t} \int d\mu(\mathbf{n}_i) \right) \left(\prod_{i=1}^{N_t} \langle \mathbf{n}(t_i) | e^{-\delta t H} | \mathbf{n}(t_{i+1}) \rangle \right) \quad (3.19)$$

with periodic boundary conditions. Here the integral measure is given by the invariant measure $d\mu(\mathbf{n}_i) = (\frac{2S+1}{4\pi}) d^3\mathbf{n}_i \delta(\mathbf{n}_i^2 - 1)$ and $\{t_i\}$ is a set of intermediate times in the imaginary-time interval $[0, \beta]$. Since δt is extremely small in the equation 3.19, it is legitimate to expand the exponent, and approximate equation 3.19 as

$$Z = \lim_{\substack{\delta t \rightarrow 0 \\ N_t \rightarrow \infty}} \left(\prod_{i=1}^{N_t} \int d\mu(\mathbf{n}_i) \right) \left(\prod_{i=1}^{N_t} [\langle \mathbf{n}(t_i) | \mathbf{n}(t_{i+1}) \rangle - \delta t \langle \mathbf{n}(t_i) | H | \mathbf{n}(t_{i+1}) \rangle] \right). \quad (3.20)$$

Within the same approximation we can write

$$\frac{\langle \mathbf{n}(t_i) | H | \mathbf{n}(t_{i+1}) \rangle}{\langle \mathbf{n}(t_i) | \mathbf{n}(t_{i+1}) \rangle} \simeq \langle \mathbf{n}(t_i) | H | \mathbf{n}(t_i) \rangle + O(\delta t). \quad (3.21)$$

Using the inner product formula 3.14, we get

$$\langle \mathbf{n}(t_i) | \mathbf{n}(t_{i+1}) \rangle = e^{i\Phi(\mathbf{n}(t_i), \mathbf{n}(t_{i+1}), \mathbf{n}_0)} \left(\frac{1 + \mathbf{n}(t_i) \cdot \mathbf{n}(t_{i+1})}{2} \right)^S \quad (3.22)$$

We now insert the equations 3.21 and 3.22 into 3.20 to find the expression for the path integral

$$Z = \lim_{\substack{\delta t \rightarrow 0 \\ N_t \rightarrow \infty}} \int \mathcal{D}\mathbf{n} e^{-S_E[\mathbf{n}]}, \quad (3.23)$$

where the measure $\mathcal{D}\mathbf{n}$ is given by

$$\mathcal{D}\mathbf{n} = \prod_{i=1}^{N_t} d\mu(\mathbf{n}(t_i)) \quad (3.24)$$

and the Euclidean action $S_E[\mathbf{n}]$ is given by

$$S_E[\mathbf{n}] = \sum_{i=1}^{N_t} \langle \mathbf{n}(t_i) | H | \mathbf{n}(t_i) \rangle - iS \sum_{i=1}^{N_t} (\Phi(\mathbf{n}(t_i), \mathbf{n}(t_{i+1}), \mathbf{n}_0)) - S \sum_{i=1}^{N_t} \ln \left(\frac{1 + \mathbf{n}(t_i) \cdot \mathbf{n}(t_{i+1})}{2} \right). \quad (3.25)$$

Throughout this derivation, we have assumed that the unit vectors $\mathbf{n}(t_i)$ follow closed trajectories (i.e $\mathbf{n}_0 = \mathbf{n}(t_{N_t+1})$) on the sphere \mathbb{S}^2 which are sufficiently smooth that all the approximations of 3.20 make sense. The continuum limit ($N_t \rightarrow \infty, \delta t \rightarrow 0$) of 3.25 gives

$$S_E[\mathbf{n}] = -iS S_{WZ}[\mathbf{n}] + \frac{S\delta t}{4} \int_0^\beta dt (\partial_t \mathbf{n}(t))^2 + S \int_0^\beta dt \mathbf{B} \cdot \mathbf{n}(t), \quad (3.26)$$

Where \mathbf{B} is an external magnetic field. The first term in 3.26 is called the Wess-Zumino action

$$S_{WZ}[\mathbf{n}] = \int_0^1 d\tau \int_0^\beta dt \mathbf{n}(t, \tau) \cdot (\partial_t \mathbf{n}(t, \tau) \times \partial_\tau \mathbf{n}(t, \tau)) \quad (3.27)$$

where $\mathbf{n}(t, \tau)$ is an arbitrary smooth parametrization of the some specific cap configuration bounded by a curve Γ . As a technical note, the sum of areas of spherical triangles defined by the term $\Phi(\mathbf{n}(t_i), \mathbf{n}(t_{i+1}), \mathbf{n}_0)$ in the Euclidean action could not be determined uniquely. This is because we can always define two types of spherical triangles formed out of the vertices $\mathbf{n}(t_i), \mathbf{n}(t_{i+1})$ and \mathbf{n}_0 . Since the unit sphere \mathbb{S}^2 has no boundary, we end up with two areas Λ_+ and Λ_- separated by the boundary Γ . The oriented area of Λ_+ and Λ_- differ by 4π , that is ,

$$\mathcal{A}(\Lambda_+) + \mathcal{A}(\Lambda_-) = 4\pi. \quad (3.28)$$

The unit vectors $\mathbf{n}(t, \tau)$ satisfy the boundary conditions

$$\mathbf{n}(t, 0) \equiv \mathbf{n}(t), \quad \mathbf{n}(t, 1) \equiv \mathbf{n}_0, \quad \mathbf{n}(0, \tau) \equiv \mathbf{n}(\beta, \tau) \quad (3.29)$$

Where $t \in [0, \beta]$ and $\tau \in [0, 1]$. We can get back to real time x_0 , with $t = ix_0$ and $\beta = iT$ where T is the imaginary time span by writing

$$Z = \int \mathcal{D}\mathbf{n} e^{iS_M[\mathbf{n}]}. \quad (3.30)$$

The Minkowskian action $S_M[\mathbf{n}]$ is given by

$$S_M[\mathbf{n}] = S S_{WZ}[\mathbf{n}] + \frac{S\delta t}{4} \int_0^T dx_0 (\partial_0 \mathbf{n}(x_0))^2 - S \int_0^T dx_0 \mathbf{B} \cdot \mathbf{n}(x_0). \quad (3.31)$$

The usual electromagnetic coupling gives a contribution to the action of the form

$$S_{em} = \oint dx_0 \mathbf{A} \cdot \frac{\partial \mathbf{n}}{\partial x_0}, \quad (3.32)$$

Where \mathbf{A} is the vector potential at position $\mathbf{n}(x_0)$. The circulation of vector field $\mathbf{A}(x_0)$ is the accumulated change in the phase of spin state under an adiabatic time evolution

$$\oint d\mathbf{n} \cdot \mathbf{A}[\mathbf{n}] = \int_0^T \langle \mathbf{n}(t) | \partial_t \mathbf{n}(t) \rangle. \quad (3.33)$$

with $|\mathbf{n}(0)\rangle = |\mathbf{n}(T)\rangle$. The vector potential $\mathbf{A}[\mathbf{n}]$ defined in such a manner is usually called the Berry connection [25].

3.3 Landau-Lifshitz-Gilbert Equation

The Landau-Lifshitz (LL)-equation fails to include dissipation effects. The experimental hysteresis curves of ferromagnetic samples show that after a certain critical value of applied magnetic field, the magnetization saturates and becomes uniform with totally parallel alignment to the direction of the applied magnetic field. Therefore, Gilbert in 1955 modified the LL equation by adding a torque -like term to incorporate this experimental fact [26]. The LLG equation takes the form

$$\dot{\mathbf{n}} = \gamma \mathbf{n} \times \mathbf{h}_{eff} - \alpha \mathbf{n} \times \dot{\mathbf{n}}. \quad (3.34)$$

where α called the Gilbert or damping constant, its value varying from 0.001 to 0.1, depending on the properties of magnetic materials. The equation 3.34 could be written alternatively by applying the LLG equation once again on the right-hand side

$$\begin{aligned} \dot{\mathbf{n}} &= \gamma \mathbf{n} \times \mathbf{h}_{eff} - \alpha \mathbf{n} \times [\gamma \mathbf{n} \times \mathbf{h}_{eff} - \alpha \mathbf{n} \times \dot{\mathbf{n}}] \\ &= \gamma \mathbf{n} \times \mathbf{h}_{eff} - \alpha \gamma \mathbf{n} \times (\mathbf{n} \times \mathbf{h}_{eff}) - \alpha^2 \dot{\mathbf{n}}, \end{aligned} \quad (3.35)$$

where we have used the vector identity $\mathbf{n} \times (\mathbf{n} \times \dot{\mathbf{n}}) = \mathbf{n} (\mathbf{n} \cdot \dot{\mathbf{n}}) - \dot{\mathbf{n}} (\mathbf{n}^2)$ to move from the first line to the second line in the previous equation using the fact that $\mathbf{n} \cdot \dot{\mathbf{n}} = 0$ and $\mathbf{n}^2 = 1$. After few straightforward algebraic steps we arrive at the desired result

$$\dot{\mathbf{n}} = \frac{\gamma}{1 + \alpha^2} [\mathbf{n} \times \mathbf{h}_{eff} - \alpha \mathbf{n} \times (\mathbf{n} \times \mathbf{h}_{eff})]. \quad (3.36)$$

with no time derivative terms appear on the right-hand side. LLG equation in this form is widely used in describing the spin dynamics of magnetic materials. For practical reasons, researchers tend to use the LLG equation written in terms of magnetization vector not the spin vector. the Magnetization form could be from the previous equations by sending $\mathbf{n} \rightarrow -\mathbf{n}$ everywhere in 3.34 and 3.36.

one can prove that the Gilbert term $\alpha \mathbf{n} \times \dot{\mathbf{n}}$ is responsible for damping by working out its energy rate of change.

The total energy for arbitrary dimension d is given by

$$E[\mathbf{n}] = \frac{\hbar S \gamma}{a^d} \int d^d \mathbf{r} H[\mathbf{n}, \partial_\mu \mathbf{n}, \mathbf{r}], \quad (3.37)$$

and its rate of change in time reads

$$\begin{aligned}
\dot{E}[\mathbf{n}] &= \frac{\hbar S \gamma}{a^d} \int d^d \mathbf{r} \frac{\delta H}{\delta \mathbf{n}} \cdot \dot{\mathbf{n}} = -\frac{\hbar S \gamma}{a^d} \int d^d \mathbf{r} \mathbf{h}_{eff} \cdot \dot{\mathbf{n}} \quad (3.38) \\
&= -\frac{\hbar S \gamma}{a^d} \int d^d \mathbf{r} \underbrace{\mathbf{h}_{eff} \cdot [\gamma(\mathbf{n} \times \mathbf{f}) - \alpha \mathbf{n} \times \dot{\mathbf{n}}]}_{=0} \\
&= \frac{\hbar S \gamma \alpha}{a^d} \int d^d \mathbf{r} \mathbf{h}_{eff} \cdot (\mathbf{n} \times \dot{\mathbf{n}}) = -\frac{\hbar S \gamma \alpha}{a^d} \int d^d \mathbf{r} (\mathbf{n} \times \mathbf{h}_{eff}) \cdot \dot{\mathbf{n}} \\
&= -\frac{\hbar S \gamma \alpha}{a^d} \int d^d \mathbf{r} \frac{1}{\gamma} \underbrace{[\dot{\mathbf{n}} + \alpha(\mathbf{n} \times \dot{\mathbf{n}})]}_{=0} \cdot \dot{\mathbf{n}} = -\frac{\hbar S \alpha}{a^d} \int d^d \mathbf{r} \dot{\mathbf{n}}^2 < 0.
\end{aligned}$$

We have employed the relation $(\mathbf{n} \times \mathbf{h}_{eff}) = \frac{1}{\gamma} [\dot{\mathbf{n}} + \alpha \mathbf{n} \times \dot{\mathbf{n}}]$ between the third and fourth steps. As a result we notice that energy is a strictly decreasing function of time under the LLG dynamics.

3.4 Skyrmions in Chiral Magnets

3.4.1 Dzyaloshinskii-Moriya (DM) Interaction

Dzyaloshinskii-Moriya interaction or anisotropy exchange interaction is an interaction between the excited state of one magnetic ion with the ground state of another magnetic ion. When acting between two spins \mathbf{S}_1 and \mathbf{S}_2 (see figure 3.4.1), it appears in the Hamiltonian as

$$H_{DM} = \mathbf{D} \cdot (\mathbf{S}_1 \times \mathbf{S}_2), \quad (3.39)$$

where \mathbf{D} called the Dzyaloshinskii-Moriya vector. It vanishes when the crystal has inversion symmetry with respect to the center between two magnetic moments. However, in general \mathbf{D} may not vanish and then will lie parallel or perpendicular to the line connecting the two spins depending on the symmetry. In 1958 I. E. Dzyaloshinskii published his work on the anisotropic exchange interaction in which he considered emergence of a uniform ferromagnetic moments in a pure antiferromagnets like α - Fe_2O_3 , MnCO_3 and CoCO_3 [28]. It is useful to emphasize the fact that Dzyaloshinskii-Moriya vector is invariant under a special class of rotation, namely the $SO(3)$, so that

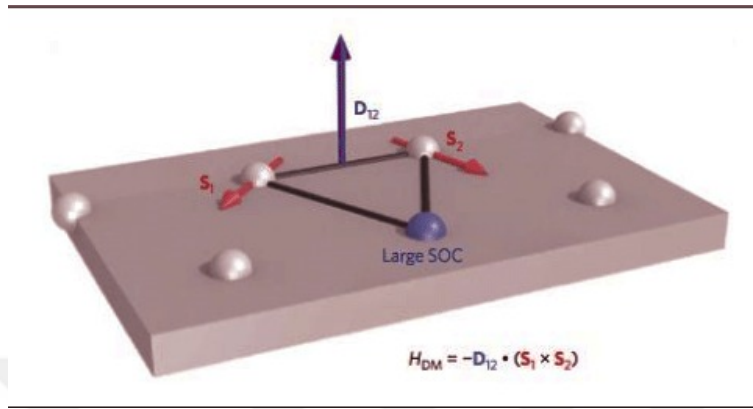


Figure 3.3: The DMI between spins \mathbf{S}_1 and \mathbf{S}_2 with DM constant D perpendicular to the line joining the two spins.

the following relation holds

$$\mathbf{D} \cdot (\mathcal{R}\mathbf{S}_1 \times \mathcal{R}\mathbf{S}_2) = \mathcal{R}\mathbf{D} \cdot (\mathcal{R}\mathbf{S}_1 \times \mathcal{R}\mathbf{S}_2) = \mathbf{D} \cdot (\mathbf{S}_1 \times \mathbf{S}_2). \quad (3.40)$$

where \mathcal{R} is a $SO(3)$ rotation matrix.

Following shortly Dzyaloshinskii's work, T.Moriya published his papers dealing with the anisotropic exchange term out of symmetry considerations [29]. Note that both Dzyaloshinskii and Moriya dealt with antiferromagnets in their papers. However, it was found later that ferromagnets with lacking inversion symmetry have non-zero DMI terms.

In cubic crystals noncentrosymmetric inversion symmetry such as MnSi, the DM interaction takes the form

$$H_{DM} = D \mathbf{S} \cdot (\nabla \times \mathbf{S}). \quad (3.41)$$

The sign of D depends solely on magnetic material characteristics. We will study this term in detail in the following section when we consider the Ginzburg-Landau theory of chiral magnets.

3.4.2 Landau Theory

The idea of treating magnetization vector \mathbf{M} as an expansion parameter is a fundamental feature of Landau theory for second-order phase transitions. It associates phase-transitions with broken symmetries. In other words, the new ground state of the system does not possess the total symmetry of the Hamiltonian. For example, in ferromagnetic materials, the rotational invariance breaks down because of spontaneous magnetization vector \mathbf{M} . Landau identified this magnetization vector which becomes nonzero below a critical temperature T_c as an order parameter. This parameter \mathbf{M} is to grow from 0 above the critical temperature T_c to a finite value below T_c . Thus near T_c , the free energy has the form

$$F = a(T - T_c)\mathbf{M}^2 + B\mathbf{M}^4, \quad (3.42)$$

where a and B are constants. Minimizing this energy with respect to the magnetization vector \mathbf{M} gives $\mathbf{M} \sim (T_c - T)^{\frac{1}{2}}$. The order-parameter represents an additional variable that must be taken into account to specify the state of system. For Heisenberg model, the order parameter is a vector with dimensionality $n = 3$, whereas for Ising model is equal to $n = 1$ since it involves only the z -component of the spin.

3.4.3 The Ginzburg-Landau (GL)- Theory

The Ginzburg-Landau theory is a continuum description of phase transitions. The main concept of this theory is based on existence of a non-zero order-parameter below a critical temperature T_c . For $T > T_c$, the order parameter vanishes. Near phase transition, the order-parameter becomes small so that one can expand the energy functional in power series of the order-parameter. Minimizing this energy functional with respect to the order-parameter gives equilibrium thermodynamic potentials of the system. In case of ferromagnetic materials or smoothly varying spin textures, the order-parameter is simply the magnetization vector $\mathbf{M}(\mathbf{r})$. In thermal equilibrium, the dimensionless free energy $G(T, B)$ written as function of both temperature T and

magnetic field B goes into the partition function as

$$Z = e^{-G} = \int \mathcal{D}\mathbf{M} e^{-F[\mathbf{M}]}, \quad (3.43)$$

where F is the energy functional depending on the order parameter \mathbf{M} . In order to calculate the free energy G we take its average value by minimizing the free energy functional with respect to the magnetization order parameter \mathbf{M}

$$G = \min_{\mathbf{M}(\mathbf{r})} F[\mathbf{M}] = F[\mathbf{M}_0]. \quad (3.44)$$

Here \mathbf{M}_0 is the minimum of free energy functional F . The leading-order corrections to the mean field are thermal Gaussian fluctuations around mean field minimum of the free energy functional

$$G \simeq F[\mathbf{M}_0] + \frac{1}{2} \ln \det \left(\frac{\delta^2 F}{\delta \mathbf{M} \delta \mathbf{M}} \right) \quad (3.45)$$

Near the critical temperature T_c , contributions from the order parameter fluctuations is comparable to its mean-field value, and this expansion becomes invalid. Near T_c , the Ginzburg-Landau energy functional for chiral magnet in term of the varying magnetization vector \mathbf{M} is

$$F[\mathbf{M}] = \int d^3r (r_0 \mathbf{M} + J(\nabla \mathbf{M})^2 + 2D \mathbf{M} \cdot (\nabla \times \mathbf{M}) + U \mathbf{M}^4 - \mathbf{B} \cdot \mathbf{M}). \quad (3.46)$$

where \mathbf{B} is the external magnetic field, r_0 , J , D and U are parameters with the conditions that both J and U are positive, (i.e. $J, U > 0$) and D is positive or negative depending on chirality of spiral spin texture. For example, the case $D > 0$ selects a left-handed spiral with wavevector $\kappa = \frac{D}{J}$. Bak and Jensen proposed a Landau-Ginzburg theory for describing emergence of large helical structures in chiral ferromagnetic materials such as MnSi and FeGe. The Landau-Ginzburg functional in the Bak-Jensen model is [30]

$$F_{\chi FM} = \frac{J}{2} (\partial_\mu \mathbf{S})^2 + \frac{u}{4} (\mathbf{S}^2 - s^2)^2 + D \mathbf{S} \cdot (\nabla \times \mathbf{S}) + F_A, \quad (3.47)$$

where

$$F_A = \frac{A_1}{2} \left[\left(\frac{\partial S_x}{\partial x} \right)^2 + \left(\frac{\partial S_y}{\partial y} \right)^2 + \left(\frac{\partial S_z}{\partial z} \right)^2 \right] + A_2 (S_x^4 + S_y^4 + S_z^4). \quad (3.48)$$

F_A is some typical spin interaction which respects the cubic crystal structure of MnSi and FeGe crystals. The relation 3.47 is a general expression up to fourth order in spins and second order in its gradients. The free energy functional part in 3.47 is identical to the classical σ -model for infinitely strong u and $s = 1$.

We can develop a theory of the spin structure that minimizes the free energy functional $F_{\chi FM}$ by considering the following Fourier transformation of the spin density near the critical temperature T_c as

$$\mathbf{S}(\mathbf{r}) = \frac{1}{\sqrt{2}} (\mathbf{S}_{\mathbf{k}} e^{i\mathbf{k}\cdot\mathbf{r}} + \mathbf{S}_{-\mathbf{k}} e^{-i\mathbf{k}\cdot\mathbf{r}}), \quad (3.49)$$

$\mathbf{S}_{\mathbf{k}}$ is some complex Fourier coefficient vector and satisfies the condition $\mathbf{S}_{\mathbf{k}} = [\mathbf{S}_{-\mathbf{k}}]^*$. Plugging 3.49 into the Bak-Jensen 3.47 and integrating over the three-dimensional space gives the free energy functional written in the momentum space

$$\begin{aligned} \langle F_{\chi FM} - F_A \rangle = & \frac{J}{2} \mathbf{k}^2 \mathbf{S}_{-\mathbf{k}} \cdot \mathbf{S}_{\mathbf{k}} + iD \mathbf{S}_{-\mathbf{k}} \cdot (\mathbf{k} \times \mathbf{S}_{\mathbf{k}}) + \\ & \frac{u}{4} (\mathbf{S}_{-\mathbf{k}} \cdot \mathbf{S}_{\mathbf{k}} - s^2)^2 + \frac{u}{8} (\mathbf{S}_{\mathbf{k}} \cdot \mathbf{S}_{\mathbf{k}}) (\mathbf{S}_{-\mathbf{k}} \cdot \mathbf{S}_{-\mathbf{k}}). \end{aligned} \quad (3.50)$$

The third term on the right-hand side of the expression 3.50 determines the magnitude of the Fourier coefficient $\mathbf{S}_{-\mathbf{k}} \cdot \mathbf{S}_{\mathbf{k}} = |\mathbf{S}_{\mathbf{k}}|^2 = s^2$, the condition $\mathbf{S}_{\mathbf{k}} \cdot \mathbf{S}_{\mathbf{k}} = 0$ justifies to drop the fourth term. It is convenient to decompose the spin density vector $\mathbf{S}_{\mathbf{k}}$ into a pair of real numbers as follows

$$\mathbf{S}_{\mathbf{k}} = \mathbf{a}_{\mathbf{k}} + i\mathbf{b}_{\mathbf{k}}. \quad (3.51)$$

The DMI term of the free energy functional then becomes

$$iD \mathbf{S}_{-\mathbf{k}} \cdot (\mathbf{k} \times \mathbf{S}_{\mathbf{k}}) = 2D \mathbf{k} \cdot (\mathbf{a}_{\mathbf{k}} \times \mathbf{b}_{\mathbf{k}}). \quad (3.52)$$

Since the size of spin $[\mathbf{S}_{\mathbf{k}}]^2 = [\mathbf{a}_{\mathbf{k}}]^2 + [\mathbf{b}_{\mathbf{k}}]^2$ fixed at s^2 , one can only adjust the relative size and orientation of $\mathbf{a}_{\mathbf{k}}$ and $\mathbf{b}_{\mathbf{k}}$ vectors in hope of maximizing the gain from DM energy. Taking $|\mathbf{a}_{\mathbf{k}}| = |\mathbf{b}_{\mathbf{k}}|$ and $\mathbf{k} \cdot (\mathbf{a}_{\mathbf{k}} \times \mathbf{b}_{\mathbf{k}}) < 0$, the first two terms of the free energy 3.50 becomes

$$J(|\mathbf{k}|^2 - 2\kappa|\mathbf{k}|)|\mathbf{a}_{\mathbf{k}}|^2 \quad (3.53)$$

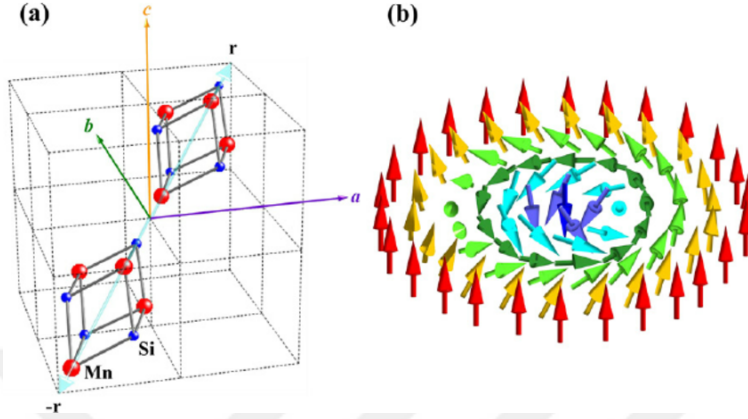


Figure 3.4: (a) MnSi structure as an example of B20 noncentrosymmetric crystal structures. (b) The Bloch-skyrmion configuration in MnSi.

where $\kappa = |\mathbf{k}| = \frac{D}{J}$ is the spiral wave-vector which is fixed by the ratio of DM and exchange energies.

Substituting the spin structure 3.49 into F_A gives

$$\frac{A_1}{2}(k_x^2|S_{\mathbf{k}x}|^2 + k_y^2|S_{\mathbf{k}y}|^2 + k_z^2|S_{\mathbf{k}z}|^2). \quad (3.54)$$

For materials such as MnSi (see figure 3.4.3 for crystal structure), the zero-field orientation of the spiral turns is $\mathbf{k}|| [111]$, which corresponds in the GL description to $A_1 < 0$. As concluding remark, we found that the spin structure minimizing the free energy functional 3.50 of the chiral ferromagnet is the right-handed spiral for positive values of DM energy(i.e $D > 0$). The period of spiral λ fixed by the DM energy through the equation

$$\frac{2\pi}{\lambda} = \kappa = \frac{D}{J}. \quad (3.55)$$

3.4.4 Derrick-Hobart Theorem

Derrick-Hobart theorem provides a necessary condition for dynamical stability of a skyrmion or any general soliton by examining the scaling property [31, 32]. In this section, we shall apply this theorem in the case of magnetic skyrmion under the

presence of DM and Zeeman interactions. Suppose there exists a soliton solution \mathbf{n}^0 to the system. We compute each contribution in the energy functional as E_H^0 , E_{DM}^0 and E_Z^0 , where H , DM and Z denote the Heisenberg exchange, Dyzaloshinskii-Moriya and Zeeman terms. Now we consider the scaling $\mathbf{n} = \mathbf{n}^0(\lambda x)$. Substituting this scaled solution into each term in the energy functional gives,

$$E(\lambda) = E_H^0 - \lambda^{-1}|E_{DM}^0| + \lambda^{-2}E_Z^0. \quad (3.56)$$

This has a unique minimum point which could be found by the relation $\lambda = \frac{2E_Z^0}{|E_{DM}^0|}$. We choose $\lambda = 1$ for consistency. It is clear that skyrmion stabilize by DMI term. When $\lambda \rightarrow \infty$, the equation 3.56 implies that a skyrmion shrinks to zero without the DMI term.

3.4.5 \mathbb{CP}^1 -Theory of a Skyrmion Crystal

Any collection of $2n$ real numbers, from x_1 to x_{2n} , could be paired up to form collection of n complex numbers as follows $z_1 = x_1 + ix_2 \dots z_n = x_{2n-1} + ix_{2n}$. If the initial set of real numbers were subject to the unit modular constraint, $\sum_{i=1}^{2n} x_i^2 = 1$, The space of such numbers defines the hypersphere \mathbb{S}^{2n-1} . The case $n = 1$ is the most trivial case and corresponds to a point on \mathbb{S}^1 which can be identified as a complex number z of unit modulus. For $n = 2$, the four numbers pair up to give

$$\mathbf{z} = \begin{pmatrix} z_1 \\ z_2 \end{pmatrix} = \begin{pmatrix} x_1 + ix_2 \\ x_3 + ix_4 \end{pmatrix}. \quad (3.57)$$

The normalization condition $\mathbf{z}^\dagger \mathbf{z} = 1$ suggests the possibility of considering \mathbf{z} as a wavefunction of spin- $\frac{1}{2}$ particle, since the physical states are invariant under phase transformation i.e. $\mathbf{z}' \rightarrow e^{if} \mathbf{z}$. It is convenient to work in the coset space $\mathbb{S}^3/\mathbb{S}^1$, as the space of allowed wavefunctions of the two-component spinor, rather than \mathbb{S}^3 itself, where $\mathbb{S}^1 \simeq U(1)$ is the space of phase transformations. Another given name for this space is **Complex Projective Space** or \mathbb{CP}^1 for short.

The explicit coordinate representation of a \mathbb{CP}^1 -field is

$$\mathbf{z} = \begin{pmatrix} \cos \frac{\theta}{2} \\ e^{i\phi} \sin \frac{\theta}{2} \end{pmatrix} \quad (3.58)$$

Besides normalization condition, \mathbf{z} satisfies this important relation $\mathbf{n} = \mathbf{z}^\dagger \sigma \mathbf{z}$. It allows us to express the geometric spin phase in a very elegant way

$$e^{iS \int dt (\cos \theta - 1)} = e^{(2iS \int dt [\mathbf{z}^\dagger \partial_t \mathbf{z}])} \quad (3.59)$$

The main advantage of using \mathbb{CP}^1 representation comes from the fact that one can use \mathbf{z} to define a gauge potential

$$a_\mu = -i\mathbf{z}^\dagger \partial_\mu \mathbf{z} = \frac{1}{2}(1 - \cos \theta) \partial_\mu \phi, \quad (3.60)$$

for any spacetime index μ . Using this gauge field, one can define the two-form field tensor (it is also called skyrmion or topological density)

$$\begin{aligned} f_{\mu\nu} &= \frac{1}{2} \mathbf{n} \cdot (\partial_\mu \mathbf{n} \times \partial_\nu \mathbf{n}) = \frac{1}{2} \sin \theta [(\partial_\mu \theta)(\partial_\nu \phi) - (\partial_\nu \theta)(\partial_\mu \phi)] \\ &= \partial_\mu a_\nu - \partial_\nu a_\mu. \end{aligned} \quad (3.61)$$

In order to make analogy with classical electrodynamics, one can re-write the above relation as

$$\frac{1}{2} \mathbf{n} \cdot (\partial_\mu \mathbf{n} \times \partial_\nu \mathbf{n}) = \varepsilon_{\mu\nu\lambda} b_\lambda, \quad (3.62)$$

where b_λ denotes the emergent magnetic field, and on the other hand, the quantity

$$\frac{1}{2} \mathbf{n} \cdot (\partial_t \mathbf{n} \times \partial_\nu \mathbf{n}) = \partial_t a_\mu - \partial_\mu a_t = e_\mu, \quad (3.63)$$

gives the emergent electric field [33].

The effective Hamiltonian for skyrmion crystal under the presence of DM and Zeeman interactions is

$$H = \frac{J}{2} (\partial_\mu \mathbf{n}) \cdot (\partial_\mu \mathbf{n}) + D \mathbf{n} \cdot (\nabla \times \mathbf{n}) - \mathbf{B} \cdot \mathbf{n}. \quad (3.64)$$

By virtue of Hopf map $\mathbf{n} = \mathbf{z}^\dagger \boldsymbol{\sigma} \mathbf{z}$, we can write the former effective Hamiltonian with respect to the spinor \mathbf{z} . The spinor \mathbf{z} can be seen as the coherent-state of spin 1/2 particles. In angle representation, the DMI term takes the form

$$\mathbf{n} \cdot (\nabla \times \mathbf{n}) = \sin \theta \cos \theta (\cos \phi \partial_x \phi + \sin \phi \partial_y \phi) + (\sin \phi \partial_x \theta - \cos \phi \partial_y \theta - \sin^2 \theta \partial_z \phi). \quad (3.65)$$

The equivalent $\mathbb{C}\mathbb{P}^1$ expression is

$$\mathbf{n} \cdot (\nabla \times \mathbf{n}) = -2\mathbf{n} \cdot \mathbf{a} - i\mathbf{z}^\dagger (\boldsymbol{\sigma} \cdot \nabla) \mathbf{z} + i(\nabla \mathbf{z}^\dagger) \cdot \boldsymbol{\sigma} \mathbf{z}, \quad (3.66)$$

where \mathbf{a} is the emergent gauge potential and has the covariant form $a_\mu = -i\mathbf{z}^\dagger \partial_\mu \mathbf{z}$. Putting all together, the full Hamiltonian (or Hamiltonian density for accuracy) takes the form

$$\begin{aligned} H &= 2J (\partial_\mu \mathbf{z}^\dagger + ia_\mu \mathbf{z}^\dagger - i\kappa \mathbf{z}^\dagger \sigma_\mu) (\partial_\mu \mathbf{z} - ia_\mu \mathbf{z} + i\kappa \mathbf{z} \sigma_\mu) - \mathbf{B} \cdot \mathbf{z}^\dagger \boldsymbol{\sigma} \mathbf{z} \\ &= 2J (D_\mu \mathbf{z}^\dagger)^\dagger (D_\mu \mathbf{z}) - \mathbf{B} \cdot \mathbf{z}^\dagger \boldsymbol{\sigma} \mathbf{z}. \end{aligned} \quad (3.67)$$

In $\mathbb{C}\mathbb{P}^1$ formulation, κ is defined as $\frac{D}{2J}$. The covariant derivative is given by

$$D_\mu = \partial_\mu - ia_\mu + i\kappa \sigma_\mu \quad (3.68)$$

The inclusion of DM interaction term was done by simply including the non-dynamic term proportional to κ in the covariant derivative. Although the term $\kappa \sigma_\mu$ is non-dynamic, it has an associated non-Abelian flux with it. This fact can be seen easily by computing the two-form field strength

$$F_{\mu\nu} = i[D_\mu, D_\nu] = f_{\mu\nu} + 2\kappa^2 \varepsilon_{\mu\nu\lambda} \sigma_\lambda. \quad (3.69)$$

Where the Abelian part of the flux $f_{\mu\nu} = \partial_\mu a_\nu - \partial_\nu a_\mu$. The simplest spin structure is for ferromagnetic phase $\mathbf{n}_0 = (0, 0, 1)$ whose equivalent $\mathbb{C}\mathbb{P}^1$ representation is $\mathbf{z}_0 = (1, 0)$ (north-pole gauge) such that $\mathbf{n}_0 = \mathbf{z}_0^\dagger \boldsymbol{\sigma} \mathbf{z}_0$ is satisfied. The most general spin structure is the spin spiral state with wavevector $\mathbf{k} = k \hat{k}$ which has the $\mathbb{C}\mathbb{P}^1$ representation

$$\mathbf{z} = e^{i \frac{(\boldsymbol{\sigma} \cdot \hat{k})(\mathbf{k} \cdot \mathbf{r})}{2}} \mathbf{z}_0, \quad (3.70)$$

$$\mathbf{n} = \mathbf{n}_0 \cos(\mathbf{k} \cdot \mathbf{r}) + (\mathbf{n}_0 \times \mathbf{k}) \sin(\mathbf{k} \cdot \mathbf{r}).$$

For a single skyrmion, $\theta(r)$ is chosen to be a smooth function of the radial coordinate r with boundary conditions $\theta(0) = \pi$ and $\theta(\infty) = 0$, and the angle ϕ to coincide with the azimuthal angle $\varphi = \arctan(\frac{y}{x})$. The vector potential for a single skyrmion is

$$\mathbf{a} = -i\mathbf{z}^\dagger \nabla \mathbf{z} = \frac{\hat{\phi}}{2r} (1 - \cos \theta(r)) = \frac{\hat{\phi}}{r} \sin^2 \frac{\theta}{2}. \quad (3.71)$$

Where $\hat{\phi} = (-\sin \varphi, \cos \varphi, 0)$. The corresponding two-dimensional Abelian flux originating from this vector potential will be

$$\nabla_2 \times \mathbf{a} = \frac{1}{2r} \sin \theta(r) \theta'(r). \quad (3.72)$$

This quantity is none other than the emergent magnetic field \mathbf{b} , since we are restricted to two dimensional case, $\nabla_2 = (\partial_x, \partial_y, 0)$. In order to solve the energy functional 2.21 explicitly, we consider the skyrmion lattice as the close-packing of single skyrmions of radius r_{Sk} forming a triangular lattice. The local spin orientation (θ, ϕ) of a single skyrmion depends on the local coordinates (r, φ) as $\phi = \varphi - \frac{\pi}{2}$ and $\theta = \theta(r)$. The total energy functional of a single skyrmion becomes [34]

$$E_{Sk} = 2J \int 2\pi r dr \left[\left(\frac{1}{2} \frac{d\theta}{dr} + \kappa \right)^2 - \kappa^2 + \frac{\kappa}{r} \sin \theta \cos \theta + \frac{1}{4r^2} \sin^2 \theta - \gamma (\cos \theta - 1) \right], \quad (3.73)$$

where $\gamma = \frac{B}{2J}$. Numerically, in order to solve the energy functional, one can introduce a hard cutoff such that $\theta(r) = 0$ for $r \geq r_{Sk}$, here r_{Sk} can be regarded as half the inter skyrmion distance on the skyrmion lattice. then the total energy functional will be

$$E_{SkX} = \frac{L^2}{2\sqrt{3} r_{Sk}^2} E_{Sk}, \quad (3.74)$$

where L is the sample size.

We give the phase diagrams of magnetic structure and spin textures in a thin film of Fe_{0.5}Co_{0.5}Si in 3.4.5.

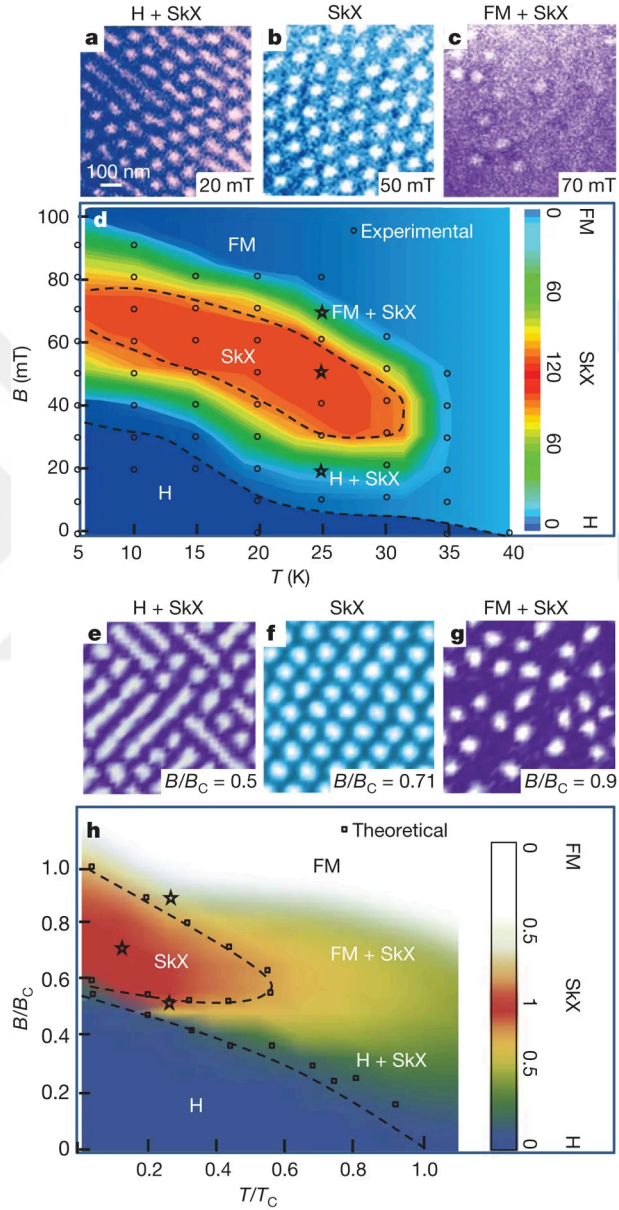


Figure 3.5: Phase diagrams of magnetic structure and spin textures in a thin film of $\text{Fe}_{0.5}\text{Co}_{0.5}\text{Si}$ in the B - T plane. H, SkX and FM denote the helical, skyrmion lattice and ferromagnetic phases respectively. B_C is the critical magnetic field for each phase, above this value the corresponding phase undergoes phase transition to the next phase in the chain $\text{H} \rightarrow \text{SkX} \rightarrow \text{FM}$. Retrieved from [35]

3.5 Skyrmion Equation of Motion Using LL Equation

The effective action for the skyrmion in terms of its center of mass coordinates $\mathbf{R} = (X, Y)$ can be expressed as [36]

$$S = -\frac{\hbar S}{a^2} \int d^2\mathbf{r} dt (1 - \cos\theta)\partial_t\phi - \int dt E[\mathbf{n}], \quad (3.75)$$

where a is the lattice spacing and $E[\mathbf{n}]$ is the energy functional given by

$$E[\mathbf{n}] = \frac{\hbar S \gamma}{a^2} \int d^2\mathbf{r} H[\mathbf{n}, \partial_\mu \mathbf{n}, \mathbf{r}]. \quad (3.76)$$

The variation of action 3.75 gives

$$\delta S = \frac{\hbar S}{a^2} \int d^2\mathbf{r} dt (\mathbf{n} \times \dot{\mathbf{n}} - \gamma \frac{\delta H}{\delta \mathbf{n}}) \cdot \delta \mathbf{n}, \quad (3.77)$$

The Euler-Lagrange equation of motion can be obtained from the previous equation through the condition $\frac{\delta S}{\delta \mathbf{n}} = 0$ which implies the continuum Landau-Lifshitz (LL)-equation

$$\mathbf{n} \times \dot{\mathbf{n}} - \gamma \frac{\delta H}{\delta \mathbf{n}} = 0. \quad (3.78)$$

We can define the force vector $\mathbf{h}_{eff} = -\frac{\delta H}{\delta \mathbf{n}}$ and rewrite the LL equation in the familiar form

$$\dot{\mathbf{n}} = \gamma \mathbf{n} \times \mathbf{h}_{eff}. \quad (3.79)$$

Specializing to the situation in which the only cause of motion is that of skyrmion coordinates \mathbf{R} allows us to write the following trial function of spin configuration

$$\mathbf{n}(\mathbf{r}, t) = \mathbf{n}(\mathbf{r} - \mathbf{R}(t)). \quad (3.80)$$

This approximation was introduced by Stone when he studied skyrmions in ferromagnets and quantum Hall systems two decades ago [37]. The variation in spin configuration $\delta \mathbf{n}$ can only be a consequence of skyrmion's displacement $\mathbf{R}(t) \rightarrow \mathbf{R}(t) + \delta \mathbf{R}(t)$. Thus, we have the following expressions

$$\delta \mathbf{n} = -(\delta X \partial_x \mathbf{n} + \delta Y \partial_y \mathbf{n}), \quad \delta \dot{\mathbf{n}} = -(\delta X \partial_x \dot{\mathbf{n}} + \delta Y \partial_y \dot{\mathbf{n}}). \quad (3.81)$$

Plugging these terms back into the geometric part of the variation 3.77 gives

$$\begin{aligned}\delta S_B &= \frac{\hbar S}{a^2} \left(\int d^2\mathbf{r} \mathbf{n} \cdot (\partial_x \mathbf{n} \times \partial_y \mathbf{n}) \right) \int dt (\dot{X} \delta Y - \dot{Y} \delta X) \\ &= \frac{2\hbar S Q_s}{a^2} \int dt (\dot{X} \delta Y - \dot{Y} \delta X).\end{aligned}\quad (3.82)$$

Applying the skyrmion ansatz $\mathbf{n}(\mathbf{r}, t) = \mathbf{n}(\mathbf{r} - \mathbf{R}(t))$ back in 3.76 gives the effective potential energy

$$\begin{aligned}V(\mathbf{R}) &= \frac{\hbar S \gamma}{a^2} \int d^2\mathbf{r} H[\mathbf{n}(\mathbf{r} - \mathbf{R}), \partial_\mu \mathbf{n}(\mathbf{r} - \mathbf{R}), \mathbf{r}] \\ &= \frac{\hbar S \gamma}{a^2} \int d^2\mathbf{r} H[\mathbf{n}(\mathbf{r}), \partial_\mu \mathbf{n}(\mathbf{r}), \mathbf{r} + \mathbf{R}].\end{aligned}\quad (3.83)$$

Collecting all terms together, the effective skyrmion Lagrangian is obtained as

$$L_s = \frac{1}{2} M_s \dot{\mathbf{R}}^2 - \frac{1}{2} G \hat{z} \cdot (\mathbf{R} \times \dot{\mathbf{R}}) - V(\mathbf{R}).\quad (3.84)$$

The quantity $G = \frac{2\hbar S Q_s}{a^2}$ is known as the gyromagnetic constant and it is widely used in skyrmion dynamics. The equation of motion becomes,

$$M_s \ddot{\mathbf{R}} = -\frac{\partial V}{\partial \mathbf{R}} + G \hat{z} \times \dot{\mathbf{R}}.\quad (3.85)$$

This is none other than Lorentz equation of motion in classical electrodynamics where the terms on right-hand side refer to electric and magnetic forces respectively. Skyrmion equation of motion was obtained from the action using Euler-Lagrange formula for the dynamical variable \mathbf{R} and its time derivative.

We shall see in the following section how to generalize the previous equation of motion to include the dissipation effects in virtue of LLG equation.

3.6 Skyrmion Equation of Motion using LLG Equation

Our previous analysis of skyrmion dynamics was based on LL equation which doesn't include a dissipation. In this section, we will derive the skyrmion equation of motion that accommodates dissipation effects.

We shall adopt a rigid skyrmion ansatz $\mathbf{n}(\mathbf{r}, t) = \mathbf{n}(\mathbf{r} - \mathbf{R}(t))$. Plugging $\dot{\mathbf{n}} = -(\dot{X}\partial_x\mathbf{n} + \dot{Y}\partial_y\mathbf{n})$ on both sides of LLG equation 3.34 gives

$$-\dot{X}\partial_x\mathbf{n} - \dot{Y}\partial_y\mathbf{n} = \gamma \mathbf{n} \times \mathbf{h}_{eff} + \alpha \mathbf{n} \times [\dot{X}\partial_x\mathbf{n} + \dot{Y}\partial_y\mathbf{n}], \quad (3.86)$$

Taking the cross product with \mathbf{n} gives,

$$-\dot{X}(\mathbf{n} \times \partial_x\mathbf{n}) - \dot{Y}(\mathbf{n} \times \partial_y\mathbf{n}) = \gamma \mathbf{n} \times \mathbf{h}_{eff} + \alpha \mathbf{n} \times [\dot{X}\partial_x\mathbf{n} + \dot{Y}\partial_y\mathbf{n}]. \quad (3.87)$$

using the identity $\mathbf{A} \times (\mathbf{B} \times \mathbf{C}) = (\mathbf{A} \cdot \mathbf{C})\mathbf{B} - (\mathbf{A} \cdot \mathbf{B})\mathbf{C}$ besides the fact that $\mathbf{n}^2 = 1$ and $\mathbf{n} \cdot \mathbf{h}_{eff} = 0$. We impose the condition that \mathbf{h}_{eff} has components in the transverse direction only. This assumption is legitimate since the force vector \mathbf{h}_{eff} enters LLG equation as a cross product term. After some algebraic manipulations and under these assumptions, the equation 3.87 becomes

$$\dot{X}(\mathbf{n} \times \partial_x\mathbf{n}) + \dot{Y}(\mathbf{n} \times \partial_y\mathbf{n}) = \gamma \mathbf{h}_{eff} + \alpha (\dot{X}\partial_x\mathbf{n} + \dot{Y}\partial_y\mathbf{n}). \quad (3.88)$$

Taking the inner product of both sides with $\partial_x\mathbf{n}$ and $\partial_y\mathbf{n}$, respectively and integrating over the whole two-dimensional space gives the following pair of equations

$$\begin{aligned} 4\pi Q_s \dot{X} &= \gamma \int d^2\mathbf{r} (\partial_y\mathbf{n} \cdot \mathbf{h}_{eff}) + 4\pi\alpha \eta \dot{Y}, \\ 4\pi Q_s \dot{Y} &= -\gamma \int d^2\mathbf{r} (\partial_x\mathbf{n} \cdot \mathbf{h}_{eff}) - 4\pi\alpha \eta \dot{X}. \end{aligned} \quad (3.89)$$

We have used the relation $\int d^2\mathbf{r} (\partial_x\mathbf{n}) \cdot (\partial_y\mathbf{n}) = 0$ and defined the shape factor η as

$$\eta = \frac{1}{4\pi} \int d^2\mathbf{r} (\partial_x\mathbf{n})^2 = \frac{1}{4\pi} \int d^2\mathbf{r} (\partial_y\mathbf{n})^2. \quad (3.90)$$

We assumed a circularly symmetric skyrmion profile. This explains why the shape factor is the same in both x and y directions. The term $\int d^2\mathbf{r} (\partial_x\mathbf{n} \cdot \mathbf{h}_{eff})$ is related to potential energy $V(\mathbf{R})$. This fact can be seen easily after some calculations

$$\begin{aligned} \int d^2\mathbf{r} (\partial_x\mathbf{n} \cdot \mathbf{h}_{eff}) &= - \int d^2\mathbf{r} \partial_x\mathbf{n} \cdot \frac{\delta H}{\delta \mathbf{n}} \\ &= - \int d^2\mathbf{r} \partial_x H + \int d^2\mathbf{r} \nabla_x H, \end{aligned} \quad (3.91)$$

where the first partial derivative acts on the implicit x dependence through \mathbf{n} and $\partial_\mu \mathbf{n}$. The second partial derivative ∇_x deals with the explicit dependence of the Hamiltonian H . The first integral vanishes since it is a total derivative, and the second integral, after shifting the position, gives

$$\begin{aligned}
& \int d^2\mathbf{r} \nabla_x H[\mathbf{n}(\mathbf{r} - \mathbf{R}), \partial_\mu \mathbf{n}(\mathbf{r} - \mathbf{R}), \mathbf{r}] \\
&= \int d^2\mathbf{r} \nabla_x H[\mathbf{n}(\mathbf{r}), \partial_\mu \mathbf{n}(\mathbf{r}), \mathbf{r} + \mathbf{R}] \\
&= \int d^2\mathbf{r} \partial_X H[\mathbf{n}(\mathbf{r}), \partial_\mu \mathbf{n}(\mathbf{r}), \mathbf{r} + \mathbf{R}] \\
&= \frac{a^2}{\hbar S \gamma} \partial_X V(\mathbf{R}),
\end{aligned} \tag{3.92}$$

where ∂_X represents the partial derivative with respect to the center coordinate X and $V(\mathbf{R})$ defines the potential energy. Putting everything together with the skyrmion mass term gives the Newtonian equation of motion

$$M_s \ddot{\mathbf{R}} = -\frac{\partial V}{\partial \mathbf{R}} + G (\hat{z} \times \dot{\mathbf{R}} - \frac{\alpha \eta}{Q_s} \dot{\mathbf{R}}). \tag{3.93}$$

It differs from 3.85 by the damping term. The quantity $\frac{\alpha \eta}{Q_s} = \tan(\theta)$ defines the skyrmion Hall angle where the sign of angle depends on the topological charge Q_s .

3.7 Stress-Energy Tensor For Magnetic Skyrmions

We consider the variational principle

$$\delta S = 0 = \delta \int d^D x L(\phi, \pi), \tag{3.94}$$

where Lagrangian density L is a function of the two classical fields $\phi(x)$ and $\pi_\alpha(x) = \partial_\alpha \phi(x)$. Given that L does not depend directly on the space-time coordinate x^α , but only indirectly through the fields $\phi(x)$ and $\pi(x)$, the conserved Noether current associated with infinitesimal space-time translations $x^\alpha \rightarrow x^\alpha + \epsilon^\alpha$ gives the stress-energy tensor $T^{\alpha\beta}$.

The variation of the Lagrangian density $\mathcal{L}(\phi, \pi)$ is given by

$$\delta L = \frac{\partial L}{\partial \phi} \delta \phi + \frac{\partial L}{\partial (\partial_\alpha \phi)} \delta \partial_\alpha \phi \tag{3.95}$$

Under spacetime translations , the variations of the fields are $\delta\phi \rightarrow \epsilon^\alpha \partial_\alpha \phi$ and $\delta\partial_\alpha \phi \rightarrow \epsilon^\beta \partial_\alpha (\partial_\beta \phi)$. Then the previous equation becomes

$$\delta L = \frac{\partial L}{\partial \phi} \epsilon^\alpha \partial_\alpha \phi + \frac{\partial L}{\partial (\partial_\alpha \phi)} \epsilon^\beta \partial_\alpha (\partial_\beta \phi). \quad (3.96)$$

Using integration by part for the second term in (3.96), we finally obtain

$$\delta L = \epsilon^\nu \underbrace{\left[\frac{\partial \mathcal{L}}{\partial \phi} - \partial_\alpha \frac{\partial L}{\partial (\partial_\alpha \phi)} \right]}_{\text{Euler-Lagrange equation}=0} \partial_\beta \phi + \epsilon^\beta \partial_\alpha \frac{L}{\partial (\partial_\alpha \phi)} \partial_\beta \phi, \quad (3.97)$$

so that

$$\delta L = \epsilon^\beta \partial_\alpha \frac{L}{\partial (\partial_\alpha \phi)} \partial_\beta \phi. \quad (3.98)$$

Since Lagrangian transforms like a scalar, $\delta L = \epsilon^\alpha \partial_\alpha L$,

$$\epsilon^\nu \eta_{\alpha\beta} \partial_\alpha L = \epsilon^\beta \partial_\alpha \frac{L}{\partial (\partial_\alpha \phi)} \partial_\beta \phi \quad (3.99)$$

we set the conservation law

$$\partial_\alpha \left[\underbrace{\frac{L}{\partial (\partial_\alpha \phi)} \partial_\beta \phi - g^{\alpha\beta} L}_{\text{Stress-energy tensor}} \right] = 0 \quad (3.100)$$

Where

$$\boxed{T^{\alpha\beta} = \frac{L}{\partial (\partial_\alpha \phi)} \partial_\beta \phi - g^{\alpha\beta} L} \quad (3.101)$$

here $g^{\alpha\beta}$ is the metric tensor and α, β run over space-time coordinates while μ, ν are for space coordinates only.

As a practical example, let us apply this machinery for calculating the stress-energy tensor for Klein-Gordon scalar field in four-dimensions. The Klein-Gordon action is given by

$$S = \int d^4 x \left[\frac{1}{2} \partial_\alpha \phi \partial^\alpha \phi - \frac{1}{2} m^2 \phi^2 \right]. \quad (3.102)$$

We compute the stress-energy tensor from 3.101, and find

$$T^{\alpha\beta} = \partial^\alpha \phi \partial^\beta \phi - \frac{1}{2} (\partial_\gamma \phi \partial^\gamma \phi - m^2 \phi^2) g^{\alpha\beta}. \quad (3.103)$$

To prove that this is indeed a conserved quantity we compute its divergence

$$\begin{aligned}
\partial_\alpha T^{\alpha\beta} &= \partial_\alpha \left[\partial^\alpha \phi \partial^\beta \phi - \frac{1}{2} (\partial_\gamma \phi \partial^\gamma \phi - m^2 \phi^2) g^{\mu\nu} \right] \\
&= \square \phi \partial^\beta \phi + \partial^\alpha \partial_\alpha \partial^\beta \phi - \frac{\partial^\beta}{2} (\partial_\gamma \partial^\gamma \phi - m^2 \phi^2) \\
&= \underbrace{(\square \phi + m^2)}_{\text{Klein-Gordon equation}=0} \partial^\beta \phi + \underbrace{\partial^\alpha \partial_\alpha \partial^\beta \phi - \partial^\beta \partial_\gamma \phi \partial^\gamma \phi}_{\text{has the same structure}=0} = 0
\end{aligned} \tag{3.104}$$

Thus the stress tensor is symmetric and it is conserved.

We wish now to find the stress-energy tensor for magnetic skyrmions. This quantity is going to be extremely useful for the symmetry analysis of magnetic skyrmions. The Heisenberg-Dzyaloshinskii-Moriya -Zeeman (HDMZ) Lagrangian is defined by

$$L = L_B - H = -S \mathbf{A} \cdot \dot{\mathbf{n}} - \frac{J}{2} (\partial_\mu \mathbf{n})^2 + D \mathbf{n} \cdot (\nabla \times \mathbf{n}) - \mathbf{B} \cdot \mathbf{n}, \tag{3.105}$$

where the term $L_B = -S(1 - \cos \theta) \partial_t \phi = -S \mathbf{A} \cdot \dot{\mathbf{n}}$ determines the Berry phase contribution. The HDMZ action remains invariant with respect to the translation of space coordinates $\mathbf{r} \rightarrow \mathbf{r} + \delta \mathbf{r}$, given that the Zeeman field is uniform $\mathbf{B}(\mathbf{r}) = \mathbf{B}$. We assume the Hamiltonian to be not explicitly dependent on time. This assumption implies the invariance of action with respect to time translation $t \rightarrow t + \delta t$ too. The variation of \mathbf{n} is [38]

$$\delta \mathbf{n} = (\delta \mathbf{r} \cdot \nabla + \delta t \partial_t) \mathbf{n} = \delta x_\alpha \partial_\alpha \mathbf{n}. \tag{3.106}$$

Using this information we can compute the variation of action S as

$$\delta S = \delta x_\beta \int d^2 \mathbf{r} dt \partial_\alpha (\delta^{\alpha\beta} L - \frac{\partial L}{\partial (\partial_\alpha \mathbf{n})} \cdot \partial_\beta \mathbf{n}) = 0 \tag{3.107}$$

The conservation law arising from this spacetime translational symmetry is $\partial_\alpha T^{\alpha\beta} = 0$ where the stress-energy tensor is defined as

$$T_{\alpha\beta} = \frac{\partial L}{\partial (\partial_\alpha \mathbf{n})} \cdot \partial_\beta \mathbf{n} - \delta_{\alpha\beta} L. \tag{3.108}$$

From the definition of $T_{\alpha\beta}$ we find

$$T_{\mu 0} = - \frac{\partial H}{\partial (\partial_\mu \mathbf{n})} \cdot \dot{\mathbf{n}}. \tag{3.109}$$

and the temporal component of the stress-energy tensor as

$$T_{00} = -\frac{\partial H}{\partial(\dot{\mathbf{n}})} \cdot \dot{\mathbf{n}} = -S\mathbf{A} \cdot \mathbf{n} = H. \quad (3.110)$$

The temporal component of stress-energy tensor is the Hamiltonian density as expected. Next let us discuss the situation when we have two spatial coordinates μ and ν . This could be done as follows:

$$T_{\mu\nu} = -\frac{\partial H}{\partial(\partial_\mu \mathbf{n})} + \delta_{\mu\nu}H - \delta_{\mu\nu}L_B = -T_{\mu\nu}^s - \delta_{\mu\nu}L_B, \quad (3.111)$$

where $T_{\mu\nu}^s$ represents the static stress-energy tensor which is defined in terms of the Hamiltonian density only with divergence equals to

$$\partial_\mu T_{\mu\nu}^s = S[\partial_\nu(\mathbf{A} \cdot \partial_t \mathbf{n}) - \partial_t(\mathbf{A} \cdot \partial_\nu \mathbf{n})]. \quad (3.112)$$

Invariance of Lagrangian density with respect to time translation implies conservation of energy while invariance with respect to space translations implies conservation of momentum.

3.8 Skyrmion Equation of Motion from Field-Theory Approach

Being a topological Soliton, skyrmion dynamics can be described gently using the field theory methods developed many years ago[39]. We shall use the emergent electrodynamics notion during the following treatment. In this approach, the emergent magnetic field is given by

$$b_\mu = \frac{1}{4}\varepsilon_{\mu\nu\lambda} \mathbf{n} \cdot (\partial_\mu \mathbf{n} \times \partial_\lambda \mathbf{n}) = \varepsilon_{\mu\nu\lambda} \partial_\nu a_\lambda. \quad (3.113)$$

Our strategy is to explore the time evolution of the emergent magnetic field. The time variation of b_μ will help us figure out the dynamics of skyrmion. Using Landau-Lifshitz equation $\dot{\mathbf{n}} = \gamma \mathbf{n} \times \mathbf{h}_{eff}$ (no damping term), we find the temporal dynamics of b_μ to be governed by the equation

$$\partial_t b_\mu = \frac{\gamma}{2} \varepsilon_{\mu\nu\lambda} \partial_\lambda \mathbf{n} \cdot \partial_\nu \mathbf{h}_{eff} = -\frac{\gamma}{2} \varepsilon_{\mu\nu\lambda} \partial_\nu (\partial_\lambda \mathbf{n} \cdot \mathbf{h}_{eff}) = -\partial_\nu J_{\mu\nu}. \quad (3.114)$$

The previous result (i.e. $\partial_t b_\mu + \partial_\nu J_{\mu\nu} = 0$) has the appearance of continuity equation reflecting conservation of the flux $\int d^3\mathbf{r} b_\mu$ regardless of the details of spin Hamiltonian. Our task now is to use the topological continuity equation during the derivation of skyrmion equation of motion.

The topological current $J_{\mu\nu}$ in 3.114 is given by

$$J_{\mu\nu} = \frac{\gamma}{2} \varepsilon_{\mu\nu\lambda} \partial_\lambda \mathbf{n} \cdot \mathbf{h}_{eff}. \quad (3.115)$$

The vector \mathbf{h}_{eff} is defined as the variational derivative of Hamiltonian with respect to magnetic moment vector, $\mathbf{h}_{eff} = -\frac{\delta H}{\delta \mathbf{n}}$. Whenever the energy density functional H does not have any explicit coordinate dependence, $H = H[\mathbf{n}, \partial_\mu \mathbf{n}]$, one can calculate \mathbf{h}_{eff} using the standard variational calculus techniques:

$$\mathbf{h}_{eff} = -\frac{\delta H}{\delta \mathbf{n}} = \partial_\mu \left[\frac{\partial H}{\partial (\partial_\mu \mathbf{n})} \right] - \frac{\partial H}{\partial \mathbf{n}}. \quad (3.116)$$

Plugging \mathbf{h}_{eff} in 3.115 gives the expression

$$J_{\mu\nu} = \frac{\gamma}{2} \varepsilon_{\mu\nu\lambda} \partial_\lambda \mathbf{n} \cdot \mathbf{h}_{eff} = \frac{\gamma}{2} \varepsilon_{\mu\nu\rho} \partial_\rho \left[\frac{\partial H}{\partial (\partial_\rho \mathbf{n})} \cdot \partial_\lambda \mathbf{n} - \delta_{\lambda\rho} H \right]. \quad (3.117)$$

We see that $J_{\mu\nu}$ appears as a total derivative of stress-energy $T_{\rho\lambda}$

$$T_{\rho\lambda} = \frac{\partial H}{\partial (\partial_\rho \mathbf{n})} \cdot \partial_\lambda \mathbf{n} - \delta_{\rho\lambda} H. \quad (3.118)$$

Since $J_{\mu\nu} = \frac{\gamma}{2} \varepsilon_{\mu\nu\lambda} \partial_\rho T_{\rho\lambda}$, the space integral $\int d^3\mathbf{r} J_{\mu\nu}$ vanishes for suitable boundary conditions imposed on $J_{\mu\nu}$ at spatial infinity. As a result, the skyrmion center coordinate remains stationary for the given form of the energy density functional which explicitly depends on both \mathbf{n} and $\partial_\mu \mathbf{n}$. In order to have a mobile guiding center, one should promote the energy density functional to become position dependent.

$$\mathcal{H}[\mathbf{n}, \partial_\mu \mathbf{n}] \rightarrow H[\mathbf{n}, \partial_\mu \mathbf{n}, \mathbf{r}]. \quad (3.119)$$

The Stress-energy tensor will change due to this inhomogeneity in the following manner

$$J_{\mu\nu} = \frac{\gamma}{2} \varepsilon_{\mu\nu\lambda} \partial_\rho T_{\rho\lambda} + \frac{\gamma}{2} \varepsilon_{\mu\nu\lambda} \nabla_\lambda H, \quad (3.120)$$

where ∇_λ is a partial derivative operator that acts on the explicit position dependent terms in H only.

Plugging the Landau-Lifshitz equation $\dot{\mathbf{n}} = \gamma \mathbf{n} \times \mathbf{h}_{eff}$ into 3.115, the topological current becomes

$$J_{\mu\nu} = \frac{\gamma}{2} \varepsilon_{\mu\nu\lambda} \partial_\lambda \mathbf{n} \cdot \mathbf{h}_{eff} = \frac{1}{2} \varepsilon_{\mu\nu\lambda} \mathbf{n} \cdot (\partial_\lambda \mathbf{n} \times \partial_t \mathbf{n}) = \partial_t a_\lambda - \partial_\lambda a_t = -\varepsilon_{\mu\nu\lambda} e_\lambda. \quad (3.121)$$

where e_λ denotes the emergent electric field. Thus, the topological current is equivalent to the emergent electric case in the non-damping case. The topological continuity equation 3.114 becomes

$$\partial_t \mathbf{b} = \nabla \times \mathbf{e}, \quad (3.122)$$

The last result is none other than the famous Faraday law for the emergent electromagnetic fields (\mathbf{e} , \mathbf{b}). We conclude that topological continuity equation is equivalent to the Faraday law of emergent electrodynamics.

In two-dimensional space, the skyrmion center coordinate is defined as

$$\mathbf{R} = (X, Y) = \frac{\int d^2\mathbf{r} \mathbf{r} b(\mathbf{r})}{\int d^2\mathbf{r} b(\mathbf{r})}. \quad (3.123)$$

The denominator in previous equation is simply a topological number that equals $2\pi Q_s$, where Q_s is known as skyrmion number. Then the topological continuity equation 3.115 simplifies and takes the form

$$\partial_t b + \nabla \cdot \mathbf{J} = 0, \quad (3.124)$$

Where the two-dimensional topological current \mathbf{J} is defined as $\mathbf{J} = (J_{31}, J_{32})$. Taking the time derivative of \mathbf{R} gives

$$2\pi \dot{\mathbf{R}} = \int d^2\mathbf{r} \mathbf{r} \dot{b} = - \int d^2\mathbf{r} \mathbf{r} (\nabla \cdot \mathbf{J}) = \int d^2\mathbf{r} \mathbf{J}. \quad (3.125)$$

It can be seen easily from this equation that the skyrmion dynamics depends on the spatial integral of the topological current \mathbf{J} . Since the homogeneous part of the stress-energy tensor fails to give the required dynamics of \mathbf{R} , we focus on the inhomogeneous

term in 3.120 which gives rise to the dynamics of skyrmion. In particular, the two-dimensional topological current (J_{31}, J_{32}) represents the inhomogeneous term

$$\mathbf{J}_{inh.} = \frac{\gamma}{2}(\nabla_y H, -\nabla_x H) = -\frac{\gamma}{2}\hat{z} \times \nabla_{\mathbf{r}} H. \quad (3.126)$$

Where $\nabla_x H$ and $\nabla_y H$ are the partial derivatives of H act only on the explicit coordinate dependence. Inserting the previous inhomogeneous contribution of \mathbf{J} into 3.125 leads to

$$\begin{aligned} 4\pi Q_s \dot{\mathbf{R}} &= -\gamma \hat{z} \times \int d^2\mathbf{r} \nabla_{\mathbf{r}} H \\ &= -\gamma \hat{z} \times \frac{\partial}{\partial \mathbf{R}} \int d^2\mathbf{r} H[\mathbf{r}, \partial_{\mu} \mathbf{n}, \mathbf{r} + \mathbf{R}] \\ &= -\frac{a^2}{\hbar S} \hat{z} \times \frac{\partial V}{\partial \mathbf{R}}, \end{aligned} \quad (3.127)$$

The previous result is nothing other than the massless limit of skyrmion dynamics 3.85 derived from the field theory perspective.

As a final note in this section, in the case of damping (i.e. Gilbert constant $\alpha \neq 0$), the topological conservation law 3.114 is still valid but with $\gamma \mathbf{h}_{eff}$ replaced by $\gamma \mathbf{h}_{eff} - \alpha \mathbf{n} \times \mathbf{h}_{eff}$. As a result, the skyrmion number Q_s remains conserved even in the presence of Gilbert damping.

3.9 LLG Equation and Spin-Transfer Torque (STT)

In non-ferromagnetic materials, spins take a random orientation in space. Electrons carry charge only in electric circuits. However, for ferromagnetic materials, the story is quite different. The outer-shell spins are oriented in the same direction. Thus, electric currents in these materials are partially polarized. Due to the interaction between ferromagnets and moving electrons, the orientation of magnetization will determine the amount of current flow. Also, the electron spins can influence the orientations of magnetizations and this is what we call a spin-transfer torque effect. In this case, we need to generalize the LLG equation such that it contains contributions from STT. The most general LLG equation can be written as

$$\dot{\mathbf{n}} = \mathbf{n} \times \mathbf{h}_{eff} + (\mathbf{j} \cdot \nabla) \mathbf{n} + \alpha \mathbf{n} \times \dot{\mathbf{n}} - \beta \mathbf{n} \times (\mathbf{j} \cdot \nabla) \mathbf{n}. \quad (3.128)$$

Where the second and last terms in 3.128 describe the adiabatic and non-adiabatic spin-transfer torque, respectively. The non-adiabatic term was introduced to account for small dissipative forces that break the conservation of spin in a spin-transfer process. As final note, we have scaled the constants such as γ in 3.128 to unity for simplicity.

3.10 Thiele Equation

LLG equation with STT term, 3.128 can be simplified if we assume a rigid drift of the spin texture as a whole. In this case, let us consider the following ansatz

$$\mathbf{n}(\mathbf{r}, t) = \mathbf{n}(\mathbf{r} - \mathbf{R}(t)), \quad (3.129)$$

Where $\mathbf{R}(t)$ describes the center of mass motion. The time derivative of 3.129 is given by

$$\dot{\mathbf{n}} = -(\dot{\mathbf{R}} \cdot \nabla) \mathbf{n}. \quad (3.130)$$

Plugging 3.129 and 3.130 into 3.128 gives,

$$-(\dot{\mathbf{R}} \cdot \nabla) \mathbf{n} = (\mathbf{j} \cdot \nabla) \mathbf{n} - \mathbf{n} \times \frac{\delta H}{\delta \mathbf{n}} + \alpha [-(\dot{\mathbf{R}} \cdot \nabla) \mathbf{n} \times \dot{\mathbf{n}}] - \beta \mathbf{n} \times -(\dot{\mathbf{R}} \cdot \nabla) \mathbf{n}. \quad (3.131)$$

In order to simplify the equation 3.131, let us multiply both sides by $\mathbf{n} \times$ and use the cross product identities, beside using $\mathbf{j} = -\mathbf{v}^s$ to be the velocity of spin polarized conduction electrons. It is more convenient to project the result onto translational modes, which are spontaneously broken during the formation of skyrmion lattice. After doing the mentioned steps, we get

$$(v_i^s - \dot{R}_i) \mathbf{n} \times \partial_i \mathbf{n} = -(n_i \frac{\delta H}{\delta n_i}) \mathbf{n} + \frac{\delta H}{\delta \mathbf{n}} - (\beta v_i^s - \alpha \dot{R}_i) \partial_i \mathbf{n}. \quad (3.132)$$

We multiply this equation by $\partial_j \mathbf{n}$ to get

$$\frac{\delta H}{\delta \mathbf{n}} \partial_j \mathbf{n} = (v_i^s - \dot{R}_i) (\mathbf{n}, \partial_i \mathbf{n}, \partial_j \mathbf{n}) + (\beta v_i^s - \alpha \dot{R}_i) \partial_i \mathbf{n} \partial_j \mathbf{n}. \quad (3.133)$$

Then by integrating the result over a unit cell, we obtain the final Thiele equation [40]

$$\mathbf{F} = \mathbf{G} \times (\mathbf{v}^s - \dot{\mathbf{R}}) + \Gamma_{ij} (\beta \mathbf{v}^s - \alpha \dot{\mathbf{R}}), \quad (3.134)$$

where \mathbf{G} and Γ_{ij} are the gyromagnetic vector and dissipative tensor, respectively.

They are explicitly given by

$$\begin{aligned} G_i &= \varepsilon_{ijk} \int d^2\mathbf{r} (\mathbf{n}, \partial_i \mathbf{n}, \partial_j \mathbf{n}), \\ \Gamma_{ij} &= \int d^2\mathbf{r} \partial_i \mathbf{n} \partial_j \mathbf{n}. \end{aligned} \quad (3.135)$$

The term in Thiele equation which contains the gyromagnetic vector is called the Magnus force. We will see later that this term is related directly with the topological charge when we study bilayer skyrmions.

If we consider an external magnetic field parallel to the z -direction and an in-plane spin polarized current, by symmetry considerations, dissipation tensor has the following simple form

$$\mathbf{\Gamma} = \Gamma \begin{bmatrix} 1 & 0 & 0 \\ 0 & 1 & 0 \\ 0 & 0 & 0 \end{bmatrix}, \quad (3.136)$$

and the gyromagnetic vector takes the form

$$\mathbf{G} = 4\pi Q_S \begin{bmatrix} 0 & -1 & 0 \\ 1 & 0 & 0 \\ 0 & 0 & 0 \end{bmatrix}. \quad (3.137)$$

Note that \mathbf{F} in equation 3.134 vanishes since HDMZ action is translationally invariant $\mathbf{r} \rightarrow \mathbf{r} + \delta\mathbf{r}$ given that Zeeman field is uniform. Thus, we obtain the following coupled equations

$$\begin{bmatrix} \alpha\Gamma & -4\pi Q_S \\ 4\pi Q_S & \alpha\Gamma \end{bmatrix} \begin{bmatrix} \dot{X} \\ \dot{Y} \end{bmatrix} = \begin{bmatrix} \beta\Gamma & -4\pi Q_S \\ 4\pi Q_S & \beta\Gamma \end{bmatrix} \quad (3.138)$$

This system is non-singular and always admits a unique solution of the form

$$\begin{aligned} \mathbf{v}_{Sk} &= \dot{\mathbf{R}} = (\dot{X}, \dot{Y}) \\ &= \frac{\beta}{\alpha} \mathbf{v}_s + \frac{\alpha - \beta}{\alpha^3 \left(\frac{\Gamma}{4\pi Q_S^2} \right) + \alpha} \left(\mathbf{v}_s + \frac{\alpha \Gamma}{4\pi Q_S} \hat{z} \times \mathbf{v}_s \right). \end{aligned} \quad (3.139)$$

From the last result, we observe that skyrmion's velocity \mathbf{v}_{Sk} is a combination of drag velocity \mathbf{v}_s and Magnus term proportional to the topological charge Q_S^{-1} .

3.11 Poisson Bracket Method in Magnetic Skyrmions

Magnetism is genuinely a quantum phenomena [41]. The magnetic response of many-body solids is a manifestation of the angular momentum of their constituents, namely the spin of electrons. At very low temperatures compared with T_C , the short-ranged fluctuations can be ignored. In micromagnetic literature [42], the magnetization dynamics is said to be governed by a classical hydrodynamical modes that vary smoothly on the scale of microscopic lattice.

3.11.1 Quantization Setups

The geometric quantization program starts by considering the hydrodynamical modes built from semi-classically coarse-grained spin density operator [43]

$$\hat{s}(\mathbf{r}) = \hbar \sum_i \mathbf{S}_i \delta(\mathbf{r} - \mathbf{R}_i), \quad (3.140)$$

where \mathbf{S}_i represents the vector of spin operators defined in case of electrical insulating case as $\mathbf{S}_i = (\hat{S}_i^x, \hat{S}_i^y, \hat{S}_i^z)$ at lattice position \mathbf{R}_i . The spin operators obey the standard commutation relations $[\hat{S}_i^\alpha, \hat{S}_j^\beta] = i\hbar \varepsilon_{\alpha\beta\gamma} \hat{S}_i^\gamma \delta_{ij}$, where δ_{ij} and $\varepsilon_{\alpha\beta\gamma}$ are the Kronecker delta and Levi-Civita antisymmetric tensor, respectively. We shall define the saturated spin -field density as the expectation value of the spin operators in the spin coherent -state representation of the macroscopic state of the magnet [44]

$$s \approx \langle \psi_{SC} | \hat{s}(\mathbf{r}) | \psi_{SC} \rangle. \quad (3.141)$$

With this construction, we adopt the following regularization of the Dirac delta function

$$\delta(\mathbf{r} - \mathbf{R}_i) \rightarrow \frac{\delta_{ij}}{A_c}, \quad (3.142)$$

where A_c does not necessarily correspond to the size of microscopic cell but to the short-wavelength cutoff for the continuum limit in the sample plane. Therefore, it is safe to interpret the spin operator $\hat{\mathbf{S}}_i$ as a quantum macroscopic spin rather than the microscopic spin operator. In order to assure the uniformity of magnetization vector along the z -axis, the thickness of sample film in the XY - plane should be taken infinitesimally small so that the spin-density field is purely a 2-dimensional vector acting within the sample plane. We will apply the Poisson method for obtaining the skyrmion dynamics at low-frequency limit.

3.11.2 Poisson Brackets in Planar Magnets

In a planar magnet at very low temperatures (i.e lower than the critical temperature T_C), the magnetization density saturates at some fixed value. Macroscopic variations in this magnitude are strongly effective and the short-ranged fluctuations could be safely omitted so that the continuum limit is valid. At this limit, the LL-equation [23] governs the dynamics of the spin-density field $\mathbf{s}(\mathbf{r}) = s \mathbf{n}(\mathbf{r})$

$$\dot{\mathbf{s}}(\mathbf{r}) = \mathbf{s} \times \mathbf{h}_{eff}(\mathbf{r}), \quad (3.143)$$

\mathbf{h}_{eff} is the thermodynamic conjugate force to \mathbf{s} and defined as the variational derivative of the energy functional H with respect to \mathbf{s} , $\mathbf{h}_{eff} = -\frac{\delta H}{\delta \mathbf{s}}$. The coupling with microscopic degrees of freedom introduces dissipation, described by Gilbert damping [26].

Since the spin-field density is the average of the spin operator, the classical magnetization dynamics should be expressed in a Liouville-like equation of motion where operators are represented in the Heisenberg picture. The Landau-Lifshitz equation of motion can be expressed in terms of Poisson brackets [45]

$$\dot{\mathbf{s}}(\mathbf{r}) = \{\mathbf{s}(\mathbf{r}), H\} = \int d^2\mathbf{r}' \{\mathbf{s}(\mathbf{r}), \mathbf{s}_\alpha(\mathbf{r}')\} \frac{\delta H}{\delta \mathbf{s}_\alpha(\mathbf{r}')}, \quad (3.144)$$

The Poisson bracket between the spin densities is

$$\{\mathbf{s}_\alpha(\mathbf{r}), \mathbf{s}_\beta(\mathbf{r}')\} = \varepsilon_{\alpha\beta\gamma} \mathbf{s}_\gamma(\mathbf{r}) \delta(\mathbf{r} - \mathbf{r}'). \quad (3.145)$$

The quantized version of the former Poisson brackets can be obtained using the usual identification

$$\{, \} \rightarrow -\frac{i}{\hbar} [,].$$

Since the spin-density field $s = |\mathbf{s}|$ has the same value everywhere in the space, one can define the Casimir invariant $C = \frac{|\mathbf{s}|^2}{2} = \frac{s^2}{2}$ which is a constant of motion regardless of symmetries of the spin Hamiltonian. Landau-Lifshitz equation can be extracted from the following noncanonical Hamiltonian

$$L[\mathbf{n}] = \int d^2\mathbf{r} a[\mathbf{n}] \cdot \dot{\mathbf{s}}(\mathbf{r}) - H[\mathbf{n}], \quad (3.146)$$

where $a[\hat{\mathbf{n}}]$ corresponds to the gauge field created by a monopole at the center of the sphere defined as

$$a[\mathbf{n}] = \frac{\mathbf{n}_0 \times \mathbf{n}}{1 - \mathbf{n}_0 \cdot \mathbf{n}}, \quad (3.147)$$

Here \mathbf{n}_0 gives the direction of the Dirac string connecting the center of sphere with infinitely distant monopole with opposite charge. $a[\mathbf{n}]$ should obey the equation

$$\nabla_{\mathbf{n}} \times \mathbf{a} = -\mathbf{n}. \quad (3.148)$$

The previous Lagrangian is defined everywhere in space except for the point \mathbf{n}_0 . The resulting Landau-Lifshitz Hamiltonian becomes singular at this point which corresponds to the north pole if we consider the stereographic projection of spheres defined by the constraint $s^2 = (\text{constant})$ onto the plane of generalized coordinates.

We used the term noncanonical Hamiltonian because the Poisson algebra contains more elements than the dynamical variables [46]. This unique feature of Landau-Lifshitz equation stems from the existence of Casimir invariance element. In spherical coordinates, we can write $\mathbf{n} = (\sin \theta \cos \phi, \sin \theta \sin \phi, \cos \theta)$. We notice that both ϕ and

$s \cos \theta$ form a canonical pair. i.e $\{\phi(\mathbf{r}), s \cos \theta(\mathbf{r}')\}$. This can be seen easily by applying the general formula of Poisson brackets between generalized coordinates parametrized by generic field variables $\xi = (\xi_1, \xi_2)$:

$$\{\xi_i(\mathbf{x}), \xi_j(\mathbf{y})\} = \int d\mathbf{r} \int d\mathbf{r}' \{s_\alpha(\mathbf{r}), s_\beta(\mathbf{r}')\} \frac{\delta \xi_i(\mathbf{x})}{\delta s_\alpha(\mathbf{r})} \frac{\delta \xi_j(\mathbf{y})}{\delta s_\beta(\mathbf{r}')}, \quad (3.149)$$

that holds alongside with 3.145.

The kinetic part in the Lagrangian 3.146 reduces to the well-known Wess-Zumino action [47]

$$L_{WZ} = s \int d^2\mathbf{r} \dot{\phi} (\cos \theta \pm 1), \quad (3.150)$$

where \pm corresponds to the Dirac string intersecting the north/south pole, $\mathbf{n}_0 = \pm \mathbf{z}$. Wess-Zumino term is an alternative way to write the spin Lagrangian in a very abstract form since it utilizes from the homotopy theory. More precisely, let us introduce a new coordinate τ and a fictitious vector potential a_τ along this new coordinate direction. The spin vector $\mathbf{n}(t, u)$ depends on u and t . We can choose τ such that at $\tau = 0$ the unit vector \mathbf{n} points along the north pole direction $\mathbf{n}(t, 0) = \mathbf{n}_0 = (0, 0, 1)$, and at $\tau = 1$ it points along the physical spin direction $\mathbf{n}(t, \tau = 1) = \mathbf{n}(t)$. The interpretation here is for every spin vector $\mathbf{n}(t)$ at time t , we have a trajectory of vectors that start from \mathbf{n}_0 at $\tau = 0$ and move along the great circle of the unit sphere to approach $\mathbf{n}(t)$ at $\tau = 1$. This fact gives us a legitimate reason to generalize the definition of variable θ to be $\theta(t, \tau) = t \theta(t)$ so that one has

$$\theta(t, 0) = 0, \quad (3.151)$$

$$\theta(t, 1) = \theta(t). \quad (3.152)$$

Where the first case, 3.151, corresponds to the north pole direction and the second case, 3.152, corresponds to the physical spin direction. The definition of $\phi(t)$ is the same and there is no need for any generalization i.e. $\phi(t, \tau) = \phi(t)$. This fact implies immediately the vanishing of the vector field a_τ , since $(1 - \cos \theta) \frac{\partial \phi}{\partial \tau} = 0$. In this setup, the emergent electric field 3.63 becomes

$$\frac{1}{2} \mathbf{n} \cdot (\partial_t \mathbf{n} \times \partial_\tau \mathbf{n}) = \partial_t a_\tau - \partial_\tau a_t = -\partial_\tau a_t. \quad (3.153)$$

Which is a first-order differential equation for a_t . It can be readily integrated to give the physical gauge field :

$$a_t(t, \tau = 1) \equiv a_t(t) = -\frac{1}{2} \int_0^1 d\tau \mathbf{n} \cdot (\partial_t \mathbf{n} \times \partial_\tau \mathbf{n}). \quad (3.154)$$

Moreover, its value at $\tau=0$ is zero since $\theta(t, 0) = 0$ and thus $a_t(t, 0) = (1 - \cos 0) \partial_t \phi = 0$. As a result, the geometric phase becomes a double integral (one for time t and one for the fictitious variable u):

$$e^{-2is(\int dt a_t(t))} = e^{-2is(\int dt \int_0^1 d\tau \mathbf{n} \cdot (\partial_t \mathbf{n} \times \partial_\tau \mathbf{n}))} = e^{iS_{WZ}}. \quad (3.155)$$

At low-frequency limit, skyrmion texture is assumed to move in a rigid-body fashion where its dynamics is given by

$$\dot{s} \approx \dot{R}_i \partial_i s. \quad (3.156)$$

The equation of motion for the center of skyrmion coordinate \mathbf{R} is $\dot{\mathbf{R}} = \{\mathbf{R}, V(\mathbf{R})\}$ which is identical to Thiele equation

$$4\pi s Q_S \dot{\mathbf{R}} \times \mathbf{z} = \mathbf{F}, \quad (3.157)$$

where $\mathbf{F} = -\frac{\partial V}{\partial \mathbf{R}}$ gives the generalized force vector and the potential $V(\mathbf{R}) = H(\mathbf{n}_{S_k}(\mathbf{r} - \mathbf{R}))$ should be taken as the free energy functional evaluated with skyrmion solution.

The canonical conjugate variable to \mathbf{R} is $\mathbf{\Pi} = 4\pi s Q_S \mathbf{R} \times \mathbf{z}$ defined such that $\{R_i, \Pi_j\} = \delta_{ij}$. This is indeed the generator of translations of the rigid texture,

$$\{\Pi_i, s\} = 4\pi s Q_S \varepsilon_{ij} \{R_j, s\} = \varepsilon_{ij} \varepsilon_{jk} \frac{\partial s}{\partial R_k} \approx \partial_i s_i. \quad (3.158)$$

Note that the algebra of translations is not closed since $\{\Pi_i, \Pi_j\} = 4\pi s Q_S \varepsilon_{ij}$. This fact is intimately related to the emergence of Magnus force [48].

3.12 The Interfacial DMI and Skyrmions in Thin Films

The DMI was also predicted to be present at the interface between ferromagnetic thin films (such as Co) and metals with large spin-orbit coupling (such as Pt). In this case,

the DMI can be written as

$$H_{DMI} = \sum_{\langle i,j \rangle} \mathbf{D}_{ij} \cdot (\mathbf{S}_i \times \mathbf{S}_j) \quad (3.159)$$

where \mathbf{D}_{ij} is the DM interaction vector for the atomic bond ij , \mathbf{S}_i is the atomic moment vector, and the summation is performed on neighbor pairs $\langle i, j \rangle$. In the case of magnetic thin film adjacent to high spin-orbit heavy metal, it was shown that the DM vector takes the simple formula $D \mathbf{u}_{ij} \times \hat{z}$, where \mathbf{u}_{ij} is the unit vector between the sites i and j . \hat{z} gives the direction normal to the film oriented from the high spin-orbit heavy metal layer to the magnetic ultrathin film. We assume the atomic spin direction to evolve slowly at atomic scales. This allows us to build up a continuous form for the DMI. As we deal with films that are thinner than any micromagnetic length scale, variations along the surface normal are ignored even if DMI originate from the interfaces. In this case, DMI energy is [49]

$$E_{DM} = t \int \int D \left[\left(n_x \frac{\partial n_z}{\partial x} - n_z \frac{\partial n_x}{\partial x} \right) + \left(n_y \frac{\partial n_z}{\partial y} - n_z \frac{\partial n_y}{\partial y} \right) \right] d^2 \mathbf{r}. \quad (3.160)$$

The global effect of the DMI on magnetization \mathbf{m} can be computed by the micromagnetic energy per volume as

$$E = D \cdot (n_z \partial_x n_x - n_x \partial_x n_z + n_z \partial_y n_y - n_y \partial_y n_z). \quad (3.161)$$

where the Dzyaloshinskii-Moriya constant D is inversely proportional to the thickness of film and takes a positive value for anticlockwise rotation. The existence of interfacial DMI is verified using different experimental methods such as Brillouin light scattering and propagation or nucleation of chiral magnetic domains. Large DMI is required for skyrmions to be stabilized in magnetic thin films / metals with large spin-orbit coupling. In ultrathin magnetic films with out-of-plane magnetization, the stabilization of an individual skyrmion is governed by the interplay between different interactions beside the DMI such as the exchange interaction and out-of-plane anisotropy. The exchange interaction characterized by the stiffness constant J tends to align all the spins in one direction. This is unlike out-of-plane anisotropy characterized by the anisotropy coefficient K , which tends to align the spins perpendicular

to the surface. In addition, we can also have additional contributions from magneto-static interaction and from geometrical confinement of the structure [7]. Taking these considerations into account, we write the quantum counterpart of an effective Hamiltonian for two dimensional chiral magnet as

$$H = -J \sum_i \mathbf{S}_i \cdot \mathbf{S}_j + D \sum_i e_\mu \cdot (\mathbf{S}_i \times \mathbf{S}_{i+e_\mu}) - B \sum_i S_i^z - K \sum_i (S_i^z)^2. \quad (3.162)$$

The first term represents the Heisenberg interaction between nearest adjacent spins taken on a square lattice for simplicity where i and e_μ represent the position and unit vector on that lattice, respectively. The second term is the interfacial DM interaction term, B and K are the perpendicular magnetic field and uniaxial anisotropy constant at lattice site i , respectively.

Chapter 4

QUANTUM ENTANGLEMENT

We present basic definitions of some important concepts in the quantum theory of composite systems which in turn will help us in the subsequent chapter.

4.1 Qubits and Bloch Sphere

The state of a two-level system is known as a spin- $\frac{1}{2}$ state. It can be written in the $|j, m\rangle$ basis

$$|\psi\rangle = \cos\frac{\theta}{2}|\frac{1}{2}, \frac{1}{2}\rangle + e^{i\phi}\sin\frac{\theta}{2}|\frac{1}{2}, -\frac{1}{2}\rangle. \quad (4.1)$$

Where $j = \frac{1}{2}$ and $m = \pm\frac{1}{2}$. Unlike classical bits which might take the values 0 or 1, two-level states or Qubits can take any value on a unit sphere. It is customary to represent each qubit on Bloch sphere parametrized by the unit vector $\mathbf{n} = (\sin\theta\cos\phi, \sin\theta\sin\phi, \cos\theta)^T$ where θ and ϕ can be determined from 4.1. We give a schematic diagram for Bloch sphere in 4.1

4.2 Density Operators

Quantum mechanics can be formulated using density operators rather than state vectors. For closed quantum systems, both formulations are identical and give the same results. Density operator (sometimes called density matrix) for an ensemble of pure states $\{p_i, |\psi_i\rangle\}$ is defined by the equation

$$\rho = \sum_i p_i |\psi_i\rangle\langle\psi_i|. \quad (4.2)$$

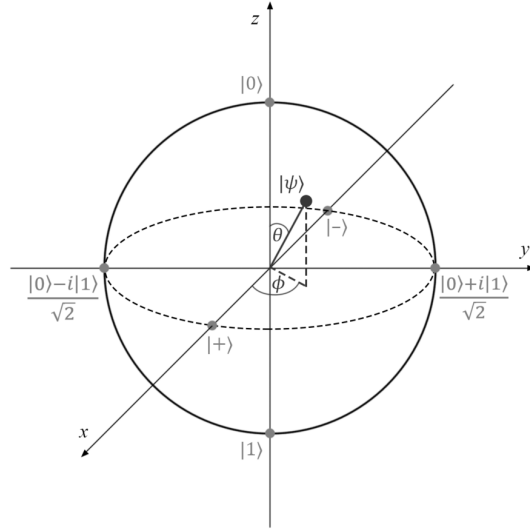


Figure 4.1: Qubit representation on Bloch sphere.

The unitary evolution of density operator if a closed quantum system is given by the action of a unitary operator U

$$\rho = \sum_i p_i |\psi_i\rangle\langle\psi_i| \rightarrow \sum_i p_i U|\psi_i\rangle\langle\psi_i|U^\dagger = U\rho U^\dagger. \quad (4.3)$$

Density operators have non-negative eigenvalues and trace equal to one i.e. $\text{Tr}(\rho) = 1$. However $\text{Tr}(\rho^2) \leq 1$ with equality if and only if ρ is pure state.

Suppose we have two physical systems A and B , whose global state is determined by a density operator ρ^{AB} . The reduced density matrix for system A is defined by

$$\rho^A = \text{Tr}_B(\rho^{AB}), \quad (4.4)$$

where Tr_B denotes the partial trace over system B . The partial trace is given by

$$\text{Tr}_B(|a_1\rangle\langle a_2| \otimes |b_1\rangle\langle b_2|) = |a_1\rangle\langle a_2| \text{Tr}(|b_1\rangle\langle b_2|). \quad (4.5)$$

where $|a_1\rangle, |a_2\rangle$ are any two state vectors in the Hilbert space \mathcal{H}_A and $|b_1\rangle, |b_2\rangle$ are any two state vectors in the Hilbert space \mathcal{H}_B . Note that $\text{Tr}|b_1\rangle\langle b_2| = \langle b_2|b_1\rangle$.

4.3 Schmidt Decomposition

Schmidt decomposition provides us with a strong tool for the study of quantum composite systems. Let $|\psi\rangle$ denote a pure state of a composite system, AB . According to Schmidt decomposition we can write the state as [50]

$$|\psi\rangle = \sum_i \lambda_i |i_A\rangle \otimes |i_B\rangle, \quad (4.6)$$

where $|i_A\rangle$ and $|i_B\rangle$ are orthonormal bases for systems A and B , respectively and λ_i are non-negative numbers satisfying $\sum \lambda_i^2 = 1$, known as Schmidt coefficients. The state $|\psi\rangle$ of a composite system is a product state if and only if it has Schmidt number equals to 1.

As a practical example, suppose $|\psi\rangle$ of a composite system with subsystems A and B . We can prove that the Schmidt number of $|\psi\rangle$ is equal to the rank of the reduced matrix ρ_A or ρ_B . From 4.6 we can calculate the outer product $|\psi\rangle\langle\psi|$ and find the reduced density matrix ρ_A as

$$\begin{aligned} \rho_A &= \text{Tr}_B(|\psi\rangle\langle\psi|) = \text{Tr}_B(\sum_i \sum_j \lambda_i \lambda_j |i_A\rangle \otimes |i_B\rangle \langle j_B| \otimes \langle j_A|) \\ &= \sum_i \sum_j \lambda_i \lambda_j |i_A\rangle \langle j_A| \text{Tr}(|i_B\rangle \langle j_B|) = \sum_i \sum_j \lambda_i \lambda_j |i_A\rangle \langle j_A| \langle j_B | i_B \rangle \\ &= \sum_i \sum_j \lambda_i \lambda_j |i_A\rangle \langle j_A| \delta_{ij} = \sum_i \lambda_i^2 |i_A\rangle \langle i_A|. \end{aligned} \quad (4.7)$$

Similarly we can prove $\rho_B = \sum_i \lambda_i^2 |i_B\rangle \langle i_B|$.

4.4 Quantum Entanglement

Quantum entanglement implies the existence of global states for composite systems which can not be written as tensor product of the states corresponding to its subsystems [51]. According to quantum mechanics, the total Hilbert space \mathcal{H} is the tensor product of the subsystem Hilbert spaces $\mathcal{H} = \otimes_{\ell=1}^n \mathcal{H}_\ell$. Then the global state of the whole system reads

$$|\psi\rangle = \sum_{i_1 \dots i_n} c_{i_1 \dots i_n} |i_1\rangle \otimes |i_2\rangle \otimes \dots \otimes |i_n\rangle. \quad (4.8)$$

This global state cannot be written in general as a product state i.e. $|\psi\rangle \neq |\psi_1\rangle \otimes |\psi_2\rangle \otimes \cdots \otimes |\psi_n\rangle$. For bipartite systems the Hilbert space $\mathcal{H} = \mathcal{H}_1 \otimes \mathcal{H}_2$ with $\dim\mathcal{H}_1 = \dim\mathcal{H}_2 = 2$ is spanned by the well-known EPR states [52]

$$\begin{aligned} |\phi^\pm\rangle &= \frac{1}{\sqrt{2}}(|0\rangle \otimes |1\rangle \pm |1\rangle \otimes |0\rangle), \\ |\chi^\pm\rangle &= \frac{1}{\sqrt{2}}(|0\rangle \otimes |0\rangle \pm |1\rangle \otimes |1\rangle). \end{aligned} \quad (4.9)$$

Remarkably if one measures the subsystem state one finds it to be $|0\rangle$ and $|1\rangle$ with equal probabilities (i.e 50:50). Although the global state is perfectly determined, we cannot determine the state of its subsystems.

4.5 Entanglement Entropy

Entanglement entropy is defined as an entanglement measure for pure states. Its value determines whether the state is separable or entangled [53]. For bipartite systems, we can use Von Neumann or Renyi entropies as entanglement measures for pure states.

Consider a quantum system consisting of two subsystems A and B . Each subsystem is characterized by a reduced density matrix ρ_A and ρ_B . The density matrix for the whole system is $\rho_{AB} = |\psi\rangle\langle\psi|$. Von Neumann entropy S is

$$S(\rho_A) = -\text{Tr}(\rho_A \log\rho_A) = -\text{Tr}(\rho_B \log\rho_B) = S(\rho_B). \quad (4.10)$$

Where $\rho_A = \text{Tr}_B(\rho_{AB})$ and $\rho_B = \text{Tr}_A(\rho_{AB})$. When either $S(A)$ or $S(B)$ equals to zero, we have a separable state. As a side note, many entanglement measures reduce to entanglement entropy such as entanglement of formation, relative entropy of entanglement. However, some entanglement measures can not be reduced to entanglement entropy such as negativity and logarithmic negativity [53].

The Renyi entanglement entropies S_α are computed using the reduced density matrices beside non-negative index called Renyi index α . It takes the form

$$S_\alpha(\rho_A) = \frac{1}{1-\alpha} \log \text{Tr}(\rho_A^\alpha) = S_\alpha(\rho_B). \quad (4.11)$$

It is not difficult to show that Renyi entropy approaches Von Neumann entropy when $\alpha \rightarrow 1$.



Chapter 5

SU(4) DESCRIPTION OF BILAYER SKYRMION-ANTISKYRMION PAIRS

We study the antiferromagnetic coupling and entanglement between skyrmion lattices in magnetic bilayer systems. We first formulate the problem of large bilayer skyrmions using $\mathbb{C}\mathbb{P}^1 \otimes \mathbb{C}\mathbb{P}^1$ theory. We have considered bilayer skyrmions under the presence of Dzyaloshinskii-Moriya (DMI) and Zeeman interactions confined in a two-dimensional chiral magnet such as $\text{Fe}_{0.5}\text{Co}_{0.5}\text{Si}$. We parametrize bilayer skyrmions using *SU*(4) representation, and represent each skyrmion and antiskyrmion using Schmidt decomposition. The reduced density matrices for the skyrmion and the antiskyrmion are calculated. The conditions for maximal, partial entanglement and separable bilayer skyrmions are presented [54].

5.1 Motivation

Skyrmions can be driven by charge or spin currents in confined geometries [55]. In general, skyrmions are subject to skyrmion Hall effect (SkHE) caused by the Magnus force. The SkHE was predicted theoretically in [56] and has been observed experimentally [57]. The SkHE is caused by Magnus force acting on the moving skyrmion with non-vanishing topological charge [48]. Magnus force is the force acting transverse to the skyrmion's velocity in the medium and can be interpreted as a manifestation of the real-space Berry phase [59].

SkHE is a detrimental effect since the skyrmions that experience it will deviate from going along a straight path. As a result, skyrmions in motion can be damaged or even destroyed at the edges of the thin film sample. One way of suppressing SkHE is to consider two perpendicular chiral thin films strongly coupled via antiferromagnetic

(AFM) exchange coupling. It is expected that when skyrmion lattice is formed at the bottom thin film, simultaneously another skyrmion lattice is created at the top thin film with opposite topological charge. In this case, total SkHE vanishes since the Magnus force acting on the top skyrmion is equal to the Magnus force that acts on the bottom skyrmion with opposite sign leaving us with zero net force. Analogous scheme was proposed to suppress SkHE in nanoscale Néel skyrmion by considering two perpendicular ferromagnetic films separated by an insulator with heavy metal underneath the second ferromagnetic film [60, 61].

Quantum signatures for large skyrmions can emerge at the phase boundary between skyrmion crystal phase (SkX) and ferromagnetic phase at zero temperature like skyrmions in $\text{Fe}_{0.5}\text{Co}_{0.5}\text{Si}$. During this phase transition, quantum liquid phase will emerge [58]. In this case, the classical LLG [26] and Thiele equation [40] break down due to quantum fluctuations. The full quantum theory of bilayer skyrmions is out of the scope of this work and it can be recovered under some circumstances. As an example, for sufficiently weak antiferromagnetic exchange coupling between thin films, bilayer skyrmion (antiferromagnetically coupled skyrmion-antiskyrmion pair) can be seen as two separate skyrmions and the quantum dynamics is already known for a single large skyrmion [58]. In this work, we give a detailed theory of large bilayer skyrmions (with sizes at order of 100 nm) using HDMZ (Heisenberg exchange, Dzyaloshinskii-Moriya and Zeeman interactions) model. We study the problem of entanglement in large bilayer skyrmions from general perspective using our developed continuum theory of bilayer skyrmions and the $SU(4)$ representation. In the final section, we study the geometry of quantum states in bilayer skyrmions.

5.2 The $\mathbb{CP}^1 \otimes \mathbb{CP}^1$ -Theory of Large Bilayer Skyrmion

We consider two thin films fabricated from chiral magnets separated by an insulating spacer with antiferromagnetic coupling between the films. We assumed each chiral film to host Bloch skyrmions under certain ranges of temperature and external magnetic field determined by the film's parameters. Skyrmions in the first thin-film are

equal in size with skyrmions in the second thin-film but with opposite topological charge. For our model to hold, we assume temperatures lower than the magnon gap and a skyrmion with large radius. Luckily, skyrmions in $\text{Fe}_{0.5}\text{Co}_{0.5}\text{Si}$ support these assumptions [35]. We present a detailed theory of bilayer skyrmions written with respect to $\mathbb{CP}^1 \otimes \mathbb{CP}^1$ -theory. The HDMZ Hamiltonian density for each chiral magnet layer is

$$\mathcal{H}_\zeta = \frac{J}{2} (\partial_\mu \mathbf{n}_\zeta) \cdot (\partial_\mu \mathbf{n}_\zeta) + D \mathbf{n}_\zeta \cdot (\nabla \times \mathbf{n}_\zeta) - \mathbf{B} \cdot \mathbf{n}_\zeta, \quad (5.1)$$

We adopted Einstein summation notation for repeated indices $\partial_\mu \mathbf{n} \cdot \partial_\mu \mathbf{n} \equiv \Sigma_\mu \partial_\mu \mathbf{n} \cdot \partial_\mu \mathbf{n}$. Since we are interested in two-dimensional thin films fabricated from chiral magnets, $\mu = (x, y)$ and $\zeta = (S, A)$ label the skyrmion and anti-Skyrmion, respectively.

$\mathbf{n}_\zeta = (\sin \theta_\zeta \cos \phi_\zeta, \sin \theta_\zeta \sin \phi_\zeta, \cos \theta_\zeta)^T$ is the transpose magnetic moment unit written in the $O(3)$ representation and has unit modulus $|\mathbf{n}_\zeta|^2 = 1$. The first term in the Hamiltonian is the exchange interaction with exchange constant J , the second term is the DMI term with D being the Dzyaloshinskii-Moriya (DM) vector constant [7]. The DMI term is responsible for chirality in the system since it has a vanishing value for centrosymmetric structures. The last term is the Zeeman interaction which plays an important role in stabilization of large skyrmions. The magnetic anisotropy term is ignored since such a term does not play an important role in $\text{Fe}_{0.5}\text{Co}_{0.5}\text{Si}$ [35]. The total energy is the spatial integral of \mathcal{H}_ζ : $H_\zeta = \int d^2r \mathcal{H}_\zeta$. The bilayer skyrmion can be described by the following Hamiltonian $H_{tot} = H_S + H_A + H_{int}$. The term H_{int} is assumed to contain the AFM exchange coupling between the two thin films

$$H_{inter} = -J_{int} \int d^2x \mathbf{n}^{\zeta=S} \cdot \mathbf{n}^{\zeta=A}. \quad (5.2)$$

The AFM interaction Hamiltonian term is responsible for the coupling between spin degrees of freedom in skyrmion and spin degrees of freedom in antiskyrmion, with AFM-coupled spins that are in opposite alignment with each other.

We will use a purely geometric approach in our investigation of quantum entanglement, thus it is more convenient to work in the equivalent \mathbb{CP}^1 formulation of the nonlinear sigma model $\text{NL}\sigma\text{M}$ [18, 34]. This can be done in virtue of the Hopf

map $\mathbf{n}_\zeta = \mathbf{z}_\zeta^\dagger \boldsymbol{\sigma} \mathbf{z}_\zeta$. This mapping connects the classical object \mathbf{n}_ζ with spinor $\mathbf{z}_\zeta = \begin{pmatrix} \cos \frac{\theta_\zeta}{2} \\ \sin \frac{\theta_\zeta}{2} e^{i\phi_\zeta} \end{pmatrix}$. The spinor \mathbf{z}_ζ can be interpreted as the coherent-state wavefunction of spin- $\frac{1}{2}$ particles. The equation 5.1 can be re-expressed in term of the spinor \mathbf{z}_ζ as (see 3.4.5 for derivation)

$$\mathcal{H}_\zeta = 2J(D_\mu \mathbf{z}_\zeta)^\dagger D_\mu \mathbf{z}_\zeta - \mathbf{B} \cdot \mathbf{z}_\zeta^\dagger \boldsymbol{\sigma} \mathbf{z}_\zeta, \quad (5.3)$$

where $D_\mu^\zeta = \partial_\mu - ia_\mu^\zeta + i\kappa\sigma_\mu^\zeta$ is the covariant derivative, $\kappa = \frac{D}{2J}$, and $a_\mu^\zeta = -i(\mathbf{z}^\dagger)^\zeta \partial_\mu \mathbf{z}^\zeta$ is the emergent gauge potential. The inclusion of DMI in the effective Hamiltonian 5.1 was done simply by adding a non-abelian gauge potential proportional to the Pauli matrices σ_μ . The emergent gauge field a_μ^ζ is usually called the real-space Berry connection. It is synthesized by adiabatically varying the magnetic texture sufficiently slow in time. The real-space Berry phase connection can give rise to the skyrmion Hall effect, unlike the momentum-space Berry connection which gives rise to the anomalous Hall effect [59]. Although the nonabelian gauge field is nondynamic (constant), it has an associated flux with it. The field tensor obtained from the gauge potential a_μ is

$$F_{\mu\nu}^\zeta = i[D_\mu^\zeta, D_\nu^\zeta] = f_{\mu\nu}^\zeta + 2\kappa^2 \epsilon_{\mu\nu\lambda} \sigma_\lambda^\zeta. \quad (5.4)$$

where the Abelian part of the flux $f_{\mu\nu}^\zeta = \partial_\mu a_\nu^\zeta - \partial_\nu a_\mu^\zeta$.

The two-dimensional emergent vector potential for the single magnetic skyrmion will be

$$\mathbf{a}^\zeta = -i\mathbf{z}_\zeta^\dagger \nabla_2 \mathbf{z}_\zeta = \frac{\hat{\phi}_\zeta}{2r} (1 - \cos \theta_\zeta(r)) = \frac{\hat{\phi}_\zeta}{r} \sin^2 \frac{\theta_\zeta}{2}, \quad (5.5)$$

where $\hat{\phi}_\zeta = (\sin \phi_\zeta, \cos \phi_\zeta, 0)$ and $\nabla_2 \equiv (\partial_x, \partial_y, 0)$. The magnetic flux originating from this vector potential will be

$$\nabla_2 \times \mathbf{a}^\zeta = \frac{1}{2r} \sin \theta_\zeta(r) \theta_\zeta'(r). \quad (5.6)$$

The local spin orientation $(\theta_\zeta, \phi_\zeta)$ is related to the local coordinate system of a single skyrmion (r, φ) such that $\theta_\zeta = \theta_\zeta(r)$ and $\phi_\zeta = \varphi_\zeta - \frac{\pi}{2}$. For the sake of simplicity, we assume $\mathbf{B} = B\hat{z} > 0$. The geometric considerations of skyrmions impose the

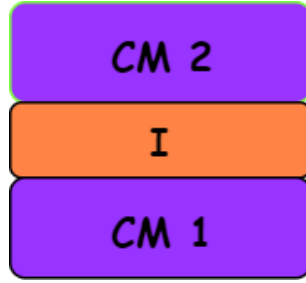


Figure 5.1: The setup used in our study consists of two identical thin films fabricated from chiral magnets (CM1,CM2) separated by an insulating material (I). The insulating material is responsible for the antiferromagnetic coupling between spins in each ferromagnetic layer. Each chiral magnet supports the emergence of large Skyrmion phase under some specific conditions of magnetic field B and temperature T .

following boundary conditions on θ_ζ : (a) $\theta_\zeta(\infty) = 0$ and (b) $\theta_\zeta(0) = \pi$. The total energy of a single skyrmion (anti-skyrmion) in the \mathbb{CP}^1 formulation reads [34]

$$E_{SK} = 4\pi J \int_0^\infty r dr \left[\left(\frac{1}{2} \frac{d\theta_\zeta}{dr} + \kappa \right)^2 - \kappa^2 + \frac{\kappa}{r} \sin \theta_\zeta \cos \theta_\zeta + \frac{1}{4r^2} \sin^2 \theta_\zeta - \gamma (\cos \theta_\zeta - 1) \right], \quad (5.7)$$

where $\gamma = \frac{B}{2J}$. Then the total energy of large bilayer skyrmion reads

$$E_{tot} = E_{Sk}(\theta_S) + E_{Sk}(\theta_A) + E_{int}(\theta_S, \theta_A), \quad (5.8)$$

In \mathbb{CP}^1 formulation, the AFM interaction term has the form

$$E_{int} = -2\pi J_{int} \int_0^\infty r dr \cos \theta_S \cdot \cos \theta_A. \quad (5.9)$$

Using calculus of variations, we find by minimizing the energy functional E_{tot} with respect to θ_S and θ_A the following equations

$$Jr \left(\frac{d\theta_S}{dr} \right)^2 + \frac{J}{r} \frac{d\theta_S}{dr} + \kappa - 2J\kappa \cos 2\theta_S - \frac{J}{2r} \sin 2\theta_S + 2J\gamma \sin \theta_S - J_{int} r \sin \theta_S \cos \theta_A = 0,$$

and

$$Jr\left(\frac{d\theta_A}{dr}\right)^2 + \frac{J}{r}\frac{d\theta_A}{dr} + \kappa - 2J\kappa\cos 2\theta_A - \frac{J}{2r}\sin 2\theta_A + 2J\gamma\sin\theta_A - J_{int}r\sin\theta_A\cos\theta_S = 0.$$

that relate θ_A and θ_S . For a sufficiently large AFM interaction, we have the case where each spin in the first film is coupled with another opposite spin in the second film. This allows us to write $\theta_A = \pi - \theta_S$ and write the total energy functional 5.8 in term of a single angle θ . Then the total energy functional 5.11 simplifies for fixed values of DM interaction constants D , exchange couplings J and magnetic fields B in both skyrmion and its AFM coupled antiskyrmion. It takes the simple form

$$E_{tot} = 4\pi J \int_0^\infty r dr \left[\left(\frac{1}{2}\frac{d\theta^S}{dr}\right)^2 + 2\gamma + \frac{1}{2r^2}\sin^2\theta^S \right] + 2\pi J_{int} \int_0^\infty r dr \cos^2\theta^S. \quad (5.10)$$

Realistically, in order for 5.7 to make sense one has to introduce a hard cutoff r_{Sk} such that $\theta_{S,A}(r) = 0$ for $r \geq r_{Sk}$. Physically, r_{Sk} is a half-Skyrmion distance in the skyrmion phase crystal or the size of a skyrmion:

$$E_{tot} = 4\pi J \int_0^{r_{Sk}} r dr \left[\left(\frac{1}{2}\frac{d\theta^S}{dr}\right)^2 + 2\gamma + \frac{1}{2r^2}\sin^2\theta^S \right] + 2\pi J_{int} \int_0^{r_{Sk}} r dr \cos^2\theta^S. \quad (5.11)$$

Throughout our study, we have considered two $\text{Fe}_{0.5}\text{Co}_{0.5}\text{Si}$ thin films separated by an insulating spacer. For $\text{Fe}_{0.5}\text{Co}_{0.5}\text{Si}$, $D = 0.48\frac{mJ}{m^2}$, the unit cell size $\approx 0.45\text{nm}$ and spiral wave length $\lambda = 90\text{nm}$. Thus, the ratio $\frac{D}{J} = \frac{2\pi a}{\lambda} \sim \frac{1}{30}$ [34, 62]. As shown in [34], the relation between $\theta(r)$ and r_{Sk} is almost a linear dependence. This allows us to expand $\theta(r)$ as a linear function of r in solving the energy functional 5.11. The coefficients of the linear function can be determined explicitly using the boundary conditions $\theta(0) = \pi$ and $\theta(r_{SK}) = 0$. We found that two dimensional emergent potential 5.5 for skyrmion and its AFM-coupled antiskyrmion has the same vector field shape as shown in 5.2. This means, both skyrmion and its AFM coupled antiskyrmion experience the same fluxes.

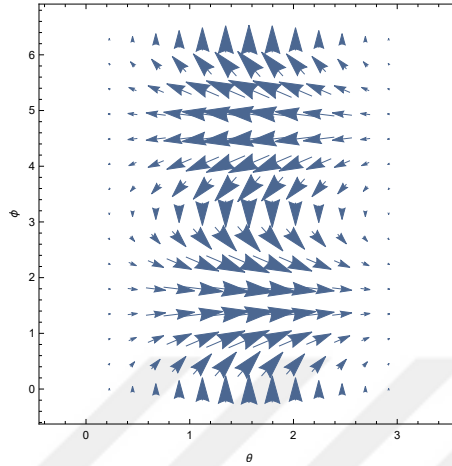


Figure 5.2: The vector field plot of emergent gauge field \mathbf{a} . We found this figure to be the same for both skyrmion and its AFM-coupled antiskyrmion. In other words, large skyrmions and its AFM coupled antiskyrmions feel the same amount of fluxes.

5.3 $SU(4)$ Parametrization of Bilayer Skyrmion

We will give a specific representation for spin degrees of freedom in bilayer skyrmions using $SU(4)$ symmetry. The $SU(4)$ skyrmions were studied before in multicomponent quantum Hall system [63] and graphene [64]. It was found that skyrmions in these systems are stabilized mainly by the competition between Zeeman and Coulomb interactions, unlike skyrmions in chiral magnets. However, both skyrmions share the same topological properties in common regardless of the systems' details. Since we have AFM coupled skyrmion-antiskyrmion pairs, our system resembles the spin-pseudospin skyrmions in term of parametrization despite the fact that one now has two skyrmions instead of one. For large bilayer skyrmions, we consider the properties of $SU(2) \otimes SU(2)$ skyrmion-antiskyrmion pairs under the presence of DM and Zeeman interactions (HDMZ model). We do this from a perspective of entanglement between the spin degrees of freedom in skyrmion and its AFM coupled anti-skyrmion. Because of Zeeman interaction term, the full $SU(4)$ symmetry breaks down to $U(1) \otimes U(1)$ symmetry where each symmetry group corresponds to a rotation of spin in the skyrmion or

antiskyrmion along the applied magnetic field direction (in our case, the z -direction). Interestingly, the DMI term written in term of spinors \mathbf{z}_ζ preserves the full $SU(4)$ symmetry. This is due to the embedding of DMI term in the covariant derivative that acts on the spinor \mathbf{z}_ζ as a nondynamic term.

We parametrize $SU(4)$ bilayer skyrmion using a Schmidt decomposition [65]. According to Schmidt decomposition, every pure state in the Hilbert space $\mathcal{H}_{12} = \mathcal{H}_1 \otimes \mathcal{H}_2$ can be written in the form

$$|\psi\rangle = \sum_{i=0}^{N-1} \lambda_i |e_i\rangle \otimes |f_i\rangle, \quad (5.12)$$

where $\{|e_i\rangle\}_{i=0}^{N_1-1}$ is an orthonormal basis for \mathcal{H}_1 , $\{|f_i\rangle\}_{i=0}^{N_2-1}$ is an orthonormal basis for \mathcal{H}_2 , $N \leq \min\{N_1, N_2\}$, and λ_i are non-negative real numbers such that $\sum_{i=0}^{N-1} \lambda_i^2 = 1$. Thus, we can express the wave-function as

$$\begin{aligned} |\Psi(\mathbf{r})\rangle &= \cos \frac{\alpha}{2} |\Phi_S^+\rangle \otimes |\Phi_A^+\rangle + \sin \frac{\alpha}{2} e^{i\beta} |\Phi_S^-\rangle \otimes |\Phi_A^-\rangle \\ &= \begin{pmatrix} \cos \frac{\alpha}{2} \cos \frac{\theta_A}{2} \cos \frac{\theta_S}{2} + \sin \frac{\theta_A}{2} \sin \frac{\theta_S}{2} e^{i(\beta - \phi_A - \phi_S)} \\ \cos \frac{\alpha}{2} \sin \frac{\theta_A}{2} \cos \frac{\theta_S}{2} e^{i\phi_A} - \sin \frac{\alpha}{2} \sin \frac{\theta_S}{2} \cos \frac{\theta_A}{2} e^{i(\beta - \phi_S)} \\ \cos \frac{\alpha}{2} \cos \frac{\theta_A}{2} \sin \frac{\theta_S}{2} e^{i\phi_S} - \sin \frac{\alpha}{2} \sin \frac{\theta_A}{2} \cos \frac{\theta_S}{2} e^{i(\beta - \phi_A)} \\ \cos \frac{\alpha}{2} \sin \frac{\theta_A}{2} \sin \frac{\theta_S}{2} e^{i(\phi_A + \phi_S)} + \sin \frac{\alpha}{2} \cos \frac{\theta_A}{2} \cos \frac{\theta_S}{2} e^{i\beta} \end{pmatrix} \end{aligned} \quad (5.13)$$

where $\alpha \in [0, \pi]$ and $\beta \in [0, 2\pi]$ are functions of \mathbf{r} , and the local two-component spinors $|\Phi_S^+\rangle, |\Phi_S^-\rangle, |\Phi_A^+\rangle$ and $|\Phi_A^-\rangle$ are constructed as follows:

$$\begin{aligned} |\Phi_\zeta^+\rangle &= \begin{pmatrix} \cos \frac{\theta_\zeta}{2} \\ \sin \frac{\theta_\zeta}{2} e^{i\phi_\zeta} \end{pmatrix}, \\ |\Phi_\zeta^-\rangle &= \begin{pmatrix} -\sin \frac{\theta_\zeta}{2} e^{-i\phi_\zeta} \\ \cos \frac{\theta_\zeta}{2} \end{pmatrix}, \end{aligned} \quad (5.14)$$

where $\theta_\zeta \in [0, \pi]$ and $\phi_\zeta \in [0, 2\pi]$ are the usual polar angles defining the vector \mathbf{n} . We can read off directly the reduced density matrices using the Schmidt decomposition. The reduced density matrices for spins in skyrmion and antiskyrmion are

$$\rho_S = \text{Tr}_A(|\Psi(\mathbf{r})\rangle\langle\Psi(\mathbf{r})|) = \cos^2 \frac{\alpha}{2} |\Phi_S^+\rangle\langle\Phi_S^+| + \sin^2 \frac{\alpha}{2} |\Phi_S^-\rangle\langle\Phi_S^-|, \quad (5.15)$$

and

$$\rho_A = \text{Tr}_S(|\Psi(\mathbf{r})\rangle\langle\Psi(\mathbf{r})|) = \cos^2 \frac{\alpha}{2} |\Phi_A^+\rangle\langle\Phi_A^+| + \sin^2 \frac{\alpha}{2} |\Phi_A^-\rangle\langle\Phi_A^-|. \quad (5.16)$$

It is convenient to express the wavefunction 5.13 as $|\Psi(\mathbf{r})\rangle = \begin{pmatrix} z_1 \\ z_2 \\ z_3 \\ z_4 \end{pmatrix}$ such that entanglement measure can be written gently as

$$\mathfrak{E} = 4|z_1 z_4 - z_2 z_3|^2. \quad (5.17)$$

For maximally entangled states we have $z_1 = z_2 = \frac{1}{\sqrt{2}}$ and $z_3 = z_4 = 0$ while for separable (factorisable) states we have $z_1 z_4 = z_2 z_3$.

Consider for simplicity the case when spins in skyrmion and antiskyrmion are maximally entangled. As an example, let $|\Phi_S^+\rangle = \begin{pmatrix} 1 \\ 0 \end{pmatrix}$, $|\Phi_A^+\rangle = \begin{pmatrix} 0 \\ 1 \end{pmatrix}$, $|\Phi_S^-\rangle = \frac{1}{\sqrt{2}} \begin{pmatrix} 1 \\ 1 \end{pmatrix}$ and $|\Phi_A^-\rangle = \frac{1}{\sqrt{2}} \begin{pmatrix} -1 \\ 1 \end{pmatrix}$. Clearly when $\alpha = \frac{\pi}{2}$, the off-diagonal terms vanish and the diagonal terms become 1. This verifies the maximal entanglement condition $\rho_{ik}^A = \frac{1}{2}\mathbb{I}_2$. In this case, it is convenient for us to use the following entanglement measure: [65]

$$\Xi := 1 - \sum_{\mu} \langle \sigma_{\mu}^2 \rangle = \sin^2 \alpha. \quad (5.18)$$

For the aforementioned example maximal entanglement corresponds to states with $\alpha = \frac{\pi}{2}$. The disentangled states correspond to the cases $\alpha = 0, \pi$. Between these two values, the reduced density matrix takes some intermediate value and can be also entangled. As shown in figure 5.3, our proposed entanglement measure is robust

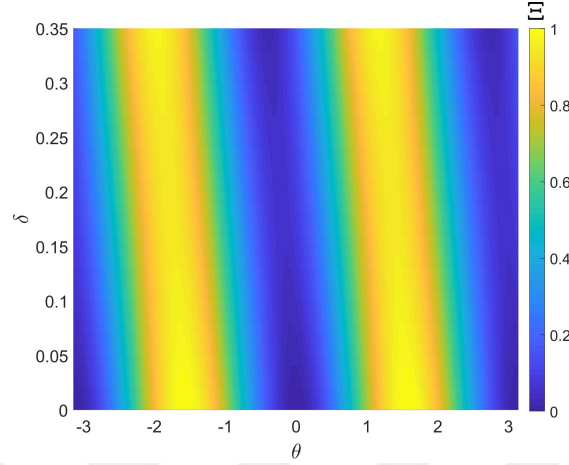


Figure 5.3: plot of entanglement measure Ξ versus angle α and small angle variation $\delta = 0 \rightarrow 0.35$ radians . Maximal entanglement happens around $\frac{\pi}{2} + n\pi$. We observe that maximally entanglement measure is robust against small angle variations.

against perturbations with small angles. This gives us a justification for using $\mathbb{C}\mathbb{P}^1 \otimes \mathbb{C}\mathbb{P}^1$ -theory. The bright regions in figure 5.3 shows the maximally entangled states.

The spin states $|\Phi_S\rangle$, $|\Phi_A\rangle$ and $|\Psi\rangle$ can be represented on Bloch spheres as shown in figure 5.3 for some specific spin states.

The local transformation operators U of the density matrices form a six-dimensional subgroup $SU(2) \otimes SU(2)$ of the full unitary group $U(4) = U(1) \otimes SU(4)$. The local transformation operators U are parametrized by an arbitrary six real variables such that $U(\theta_S, \phi_S, \theta_A, \phi_A, \alpha, \beta)^\dagger U(\theta_S, \phi_S, \theta_A, \phi_A, \alpha, \beta) = \mathbb{I}_4$ (4×4 identity matrix) . Without loss of generality, we can use $\mathbb{I}_2 \otimes \sigma_\mu$ and $\sigma_\mu \otimes \mathbb{I}_2$ as hermitian $\mathfrak{su}(2) \otimes \mathfrak{su}(2)$ Lie algebra basis of the full $SU(4)$ -bilayer skyrmion theory. Here, σ_μ and \mathbb{I}_2 denote the Pauli matrices and the two-dimensional identity matrix , respectively (see appendix B for details on $SU(4)$ basis) .

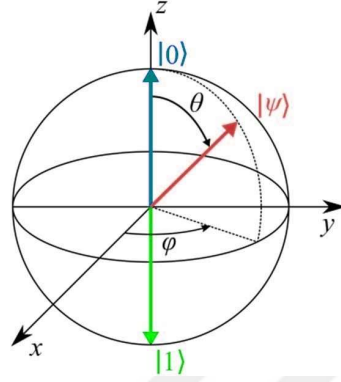


Figure 5.4: Bloch sphere representation of spin states $|\Phi_S\rangle = |0\rangle = (1\ 0)^T$, $|\Phi_A\rangle = |1\rangle = (0\ 1)^T$ and $|\Psi\rangle = (0\ \frac{1}{\sqrt{2}}\ \frac{1}{\sqrt{2}}\ 0)^T$.

5.4 Geometry of Bilayer Skyrmion

Magnetic skyrmions are whirling spin configuration augmented with topological protection against small perturbations in medium. Because magnetic skyrmions can be viewed as tensor product of large number of spin-coherent states [58]. The complete wave function of a single skyrmion can be constructed as the tensor product of spin states defined in the basis of spin-coherent representation. The skyrmion wave function corresponding to a single skyrmion will be

$$|\psi_{SC}\rangle = \sum_{i=0}^{N-1} \otimes |\mathbf{n}_i\rangle \equiv |\mathbf{n}_0\rangle \otimes |\mathbf{n}_1\rangle \otimes \dots \otimes |\mathbf{n}_{N-1}\rangle. \quad (5.19)$$

The subscript SC stands for semi-classical and N is the total number of spins. Here, the projection is defined as $\mathbf{n}_i \cdot \hat{\mathbf{S}}_i |\mathbf{n}_i\rangle = S |\mathbf{n}_i\rangle$ and i labels the spins that form the skyrmion. Considering the z -axis as a quantization axis, the state \mathbf{n}_i can be defined as [66]

$$\begin{aligned} |\mathbf{n}_i\rangle &= e^{-i\phi_i \hat{S}_i^z} e^{-i\theta_i \hat{S}_i^y} e^{-i\chi_i \hat{S}_i^z} |S\rangle \\ &= (\cos \frac{\alpha_i}{2})^{2S} \sum_{n=0}^{2S} e^{\beta_i(n-2S)} (\tan \frac{\alpha_i}{2})^2 \frac{(\hat{S}_i^-)^n}{n!} |S\rangle, \end{aligned} \quad (5.20)$$

where $\hat{S}_i^\pm = \hat{S}_i^x \pm i\hat{S}_i^y$. The operators \hat{S}_i^μ obey the commutator algebra $[\hat{S}_i^\mu, \hat{S}_i^\nu] = i\hbar \hat{S}_i^\rho$, with the associated uncertainty relation given by

$$\langle (\hat{S}_i^\mu)^2 \rangle \langle (\hat{S}_i^\nu)^2 \rangle \geq \frac{1}{4} \hbar^2 \langle (\hat{S}_i^\rho)^2 \rangle. \quad (5.21)$$

The equality holds for spin coherent state. Like the classical Glauber state in quantum optics, spin coherent states are minimum-uncertainty states. The entanglement spectrum for spin coherent states was investigated previously in ref. [67]. We can study the problem of entangled two skyrmions using many-body entanglement of spin chains [68]. In other words, the problem of entanglement in bilayer skyrmions is identical to entanglement problem for XXZ spin chains. In this case, we will have XXZ spin chain for skyrmion and another chain for antiskyrmion. Each spin chain is constructed from the same spinor. This gives us a justification for using continuum theory instead of the usual many-body quantum entanglement approaches for systems with large spin S . In this section, we will give a geometric description of the problem [69]. This approach will give us a better understanding to the problem of entangled spins in bilayer skyrmion. \mathbb{CP}^N is the space of rays in \mathbb{C}^{N+1} , or equivalently the space of equivalence classes of $N+1$ complex numbers, with at least one of them non-zero, under $(Z^0, Z^1, \dots, Z^N) \sim \lambda(Z^0, Z^1, \dots, Z^N)$, where $\lambda \in \mathbb{C}$ and $\lambda \neq 0$. In quantum field theory, the \mathbb{CP}^{N-1} field corresponds to N -component normalized spinor $z = (z_1, z_2, z_3, \dots, z_N)^T$ such that two vectors z and $e^{i\varphi}z$ are equivalent for arbitrary $\varphi \in \mathbb{R}$. The normalization of \mathbb{CP}^{N-1} spinor takes away two real parameters (or one complex) which explains why the space \mathbb{CP}^{N-1} correspond to \mathbb{C}^N . Any \mathbb{CP}^3 - manifold is isomorphic to $\frac{U(4)}{[U(3) \otimes U(1)]} \cong \frac{SU(4)}{[SU(3) \otimes U(1)]}$, therefore the second homotopy group is $\pi_2(\mathbb{CP}^3) = \pi_2\left\{\frac{SU(4)}{[SU(3) \otimes U(1)]}\right\} = \pi_1[SU(3) \otimes U(1)]$. Using the fact that the homotopy group for the product manifold factorizes as $\pi_k(\mathfrak{g} \otimes \mathcal{H}) = \pi_k(\mathfrak{g}) \otimes \pi_k(\mathcal{H})$ alongside with the fact that any simple Lie group \mathfrak{g} has a vanishing fundamental homotopy group (i.e $\pi_1(\mathfrak{g}) = 0$). We obtain $\pi_2(\mathbb{CP}^3) = \pi_1[SU(3)] \otimes \pi_1[U(1)] = \mathbb{Z}$ [16].

The pure state for each spin- $\frac{1}{2}$ can be described by a vector in a 2-dimensional complex vector space. In Dirac notation, this vector can be expressed as $|\Psi\rangle = \sum_{i=0}^{N-1} Z^i |i\rangle$, Where $|i\rangle$ is a given orthonormal basis. The distance D_{FS} between two states $|\Psi_1\rangle$

and $|\Psi_2\rangle$ is determined by the Fubini-Study distance [70]

$$\cos^2 D_{FS} = \frac{|\langle \Psi_1 | \Psi_2 \rangle|^2}{\langle \Psi_1 | \Psi_1 \rangle \langle \Psi_2 | \Psi_2 \rangle} = \frac{|Z_1 \cdot \bar{Z}_2|^2}{(Z_1 \cdot \bar{Z}_1)(Z_2 \cdot \bar{Z}_2)}. \quad (5.22)$$

where \bar{Z}_i is the row vector whose entries are the complex conjugates of the entries of the column vector \bar{Z}^i . The Fubini-Study metric measures the distinguishability of pure quantum states. In quantum communication theory, Fubini-Study distance is known as fidelity [69]. Since we have considered a continuum theory for describing large bilayer skyrmions in section 5.2, the distinguishability of any two arbitrary states of large skyrmion or antiskyrmion is difficult to observe. The infinitesimal form of the Fubini-Study distance approaches the metric tensor

$$ds^2 = \frac{Z \cdot \bar{Z} dZ \cdot d\bar{Z} - Z \cdot d\bar{Z} dZ \cdot \bar{Z}}{(Z \cdot \bar{Z})(Z \cdot \bar{Z})}, \quad (5.23)$$

Here $Z \cdot \bar{Z} = Z^i \bar{Z}_i$. From Fubini-Study metric, the time-energy uncertainty relation can be derived directly for each single spin [69]. As a spin-coherent state goes through a closed loop, it will gain the phase $\gamma = \oint \langle \psi(s) | \frac{d}{ds} | \psi(s) \rangle$. It was found that this phase is equal to the Riemannian curvature $K = \frac{1}{2S}$ of the phase space of spin-coherent state up to a constant. When $S = 1/2$ (like large 2D skyrmions), the curvature is equal to its maximum value $K = 1$ [70].

Any arbitrary state vector of a bipartite composite system can be expressed as

$$|\Psi\rangle = \frac{1}{\sqrt{N}} \sum_{i=0}^{N-1} \sum_{j=0}^{N-1} C_{ij} |i\rangle \otimes |j\rangle, \quad (5.24)$$

where C_{ij} is an $N \times N$ matrix with complex entries. For the 2×2 case, we have $(Z^0, Z^1, Z^2, Z^3) = (C_{00}, C_{01}, C_{10}, C_{11})$. Then the density matrix for the composite system can be written as $\rho_{ij,kl} = \frac{1}{N} C_{ij} C_{kl}^*$. Since the system is in pure state, its density matrix has rank one. Now suppose we perform an experiment in one of the two thin films, the reduced density matrix for this subsystem is the partially traced density matrix $\rho_A = \text{Tr}_B \rho := \text{Tr}_{\mathcal{H}_B} \rho$ which equals $\rho_{ik}^A = \sum_{j=0}^{N-1} \rho_{ij,kj}$. The rank of this subsystem density matrix may be greater than one. The global state of the bilayer skyrmion may be written as a product state spanned in the total Hilbert

space $\mathcal{H} = \mathcal{H}_A \otimes \mathcal{H}_B$

$$|\Psi\rangle = |\mathcal{A}\rangle \otimes |\mathcal{B}\rangle = \sum_{i=0}^{N-1} \sum_{j=0}^{N-1} (a_i |i\rangle) \otimes (b_j |j\rangle). \quad (5.25)$$

So the matrix $C_{ij} = a_i b_j$ is the dyadic product of two vectors a and b . It is not difficult to notice that such global state of this kind is disentangled or separable since the partially traced matrix and the matrix C_{ij} have rank one and the subsystems are in pure states of their own. On other hand, the maximally entangled state can be identified using the condition $\rho_{ik}^A = \frac{1}{N} \mathbb{I}_N$ which corresponds to $\sum_{j=0}^{N-1} C_{ij} C_{kj}^* = \delta_{ik}$. It means that we know nothing at all about the state of the subsystems even though the global state is precisely determined. The maximally entangled states form an orbit of the group of local unitary transformations. In our case, this group is $\frac{SU(2)}{\mathbb{Z}} = SO(3)$. This happens to be the real projective space \mathbb{RP}^3 . In general, the group $\frac{U(N)}{U(1)} = \frac{SU(N)}{\mathbb{Z}^N}$ is a Lagrangian sub-manifold of \mathbb{CP}^{N^2-1} . Between these two cases, the separable and maximally entangled cases, the Von Neumann entropy $S = -\text{Tr}(\rho_A \ln \rho_A)$ takes some intermediate value and they can be entangled.

Chapter 6

CONCLUSION

In this thesis, the problem of antiferromagnetically coupled skyrmions (bilayer skyrmion) has been studied using continuum theory approach. This was done by considering two thin films formed from the same chiral magnet separated by an insulating spacer with antiferromagnetic coupling between chiral films. Each chiral film was assumed to host Bloch skyrmions under certain range of temperatures and external magnetic fields determined by the film parameters. Skyrmions in the first thin-film are equal in size with skyrmions in the second thin-film but with opposite topological charge. For our model to hold, we assume temperatures lower than the magnon gap and skyrmion with large radii. Fortunately, skyrmions in $\text{Fe}_{0.5}\text{Co}_{0.5}\text{Si}$ support these assumptions. We give a representation for the spin degrees of freedom based on $SU(4)$ Lie group. Moreover, we have computed the density matrices for the spin degrees of freedom in skyrmion and its AFM-coupled antiskyrmion using Schmidt decomposition. Utilizing from the computed density matrices, we found the conditions for maximal or partial entanglement and separability within bilayer skyrmions [54]. The geometry of quantum states in bilayer skyrmions can be described using complex projective space $\mathbb{C}\mathbb{P}^3$ endowed with the unitary-invariant Fubini-Study metric. Geometrically, the entangled states can be described naturally using $\mathbb{C}\mathbb{P}^3$. We have two extreme cases corresponding to maximally entangled and separable states. The space for maximally entangled states happens to be the real projective space $\mathbb{R}\mathbb{P}^3$ while for separable states is simply the space $\mathbb{C}\mathbb{P}^1 \otimes \mathbb{C}\mathbb{P}^1$.

In comparison with graphene and multicomponent Hall systems, intimate relation between the entanglement conditions in large bilayer skyrmions and $SU(4)$ -skyrmions has been found. However, the system which has been investigated in this thesis is

different from those studied in Graphene and multicomponent quantum Hall systems. For example, they dealt in graphene case with spin-valley pseudospin degrees of freedom in a single skyrmion [71, 72]. In contrast, we have considered two skyrmions with AFM coupling between its internal spins. This is the reason why we used $\mathbb{C}\mathbb{P}^1 \otimes \mathbb{C}\mathbb{P}^1$ -theory instead of $\mathbb{C}\mathbb{P}^3$ -theory. However, the space of entangled states is $\mathbb{C}\mathbb{P}^3$ as expected [69, 73].

As a last comment, we propose the use of entanglement in skyrmion-antiskyrmion lattices for probing the geometric nature of quantum entanglement. This will help in turn to further understand and possibly manipulate magnetic skyrmions in performing quantum mechanical computations.

Appendix

A The Topological Charge Q_S

The topological charge of a magnetic skyrmion is given by

$$Q_S = \frac{1}{4\pi} \int d^2\mathbf{r} \mathbf{n} \cdot \left(\frac{\partial \mathbf{n}}{\partial x} \times \frac{\partial \mathbf{n}}{\partial y} \right). \quad (\text{A1})$$

This quantity counts how many times $\mathbf{n}(\mathbf{r}) = \mathbf{n}(x, y)$ wraps the unit sphere.

The radial symmetry of magnetic skyrmions allows us to write

$$\theta = \theta(r), \quad (\text{A2})$$

$$\phi(\varphi) = N\varphi + \gamma. \quad (\text{A3})$$

N and γ denote the vorticity and helicity, respectively. The magnetic unit vector is parametrized as

$$\mathbf{n} = (\sin \theta \cos \phi, \sin \theta \sin \phi, \cos \theta)^T, \quad (\text{A4})$$

where T represents the transpose matrix operation. By plugging A4 into A1 we find

$$\begin{aligned} Q_S &= \frac{1}{4\pi} \int_0^\infty dr \int_0^{2\pi} \frac{d\theta(r)}{dr} \frac{d\phi(\varphi)}{d\varphi} \sin \theta(r) \\ &= [\cos \theta(r)]_{r=0}^{r=\infty} [\phi(\varphi)]_{\varphi=0}^{\varphi=2\pi} = \pm N. \end{aligned} \quad (\text{A5})$$

The final result is obtained by considering the following boundary conditions imposed on θ : $\theta(\infty) = 0$ and $\theta(0) = \pi$.

For stabilized skyrmion at ground state, the lowest energy configuration has $N = +1$ and $\gamma = \pm \frac{\pi}{2}$ depending on the sign of Dzyaloshinskii-Moriya \mathbf{D} vector.

B $SU(4)$ Representation

The special unitary group $SU(N)$ has $(N^2 - 1)$ generators, where -1 is because of the condition $\det(M) = 1$ where M is any element from $SU(N)$. We denote the generators

as λ_A , $A = 1, 2, \dots, N^2 - 1$. We choose the following normalization condition between generators $\text{Tr}(\lambda_A \lambda_B) = 2\delta_{AB}$. Their commutator and anti-commutator are [74]

$$[\lambda_A, \lambda_B] = 2i f_{ABC} \lambda_C, \quad (\text{B1})$$

$$\{\lambda_A, \lambda_B\} = \frac{4}{N} + 2 d_{ABC} \lambda_C, \quad (\text{B2})$$

where f_{ABC} and d_{ABC} are the structure constants of $SU(N)$. For $N = 2$, $\lambda_A = \sigma_A$ (Pauli matrix) we have $f_{ABC} = \varepsilon_{ABC}$ and $d_{ABC} = 0$ in the case of $SU(2)$.

Since our developed model of bilayer skyrmions in chiral magnets is based on $SU(4)$ we will give a specific attention to this group. $SU(4)$ has 15 generators while $SU(2) \otimes SU(2)$ has 6 generators in total. Embedding $SU(2) \otimes SU(2)$ into $SU(4)$ we find the following representations for the skyrmion S and its AFM-coupled antiskyrmion A :

$$\tau_x^S = \begin{pmatrix} \sigma_x & 0 \\ 0 & \sigma_x \end{pmatrix}, \tau_y^S = \begin{pmatrix} \sigma_y & 0 \\ 0 & \sigma_y \end{pmatrix}, \tau_z^S = \begin{pmatrix} \sigma_z & 0 \\ 0 & \sigma_z \end{pmatrix}, \quad (\text{B3})$$

$$\tau_x^A = \begin{pmatrix} 0 & \mathbb{I}_2 \\ \mathbb{I}_2 & 0 \end{pmatrix}, \tau_y^A = \begin{pmatrix} 0 & -i\mathbb{I}_2 \\ i\mathbb{I}_2 & 0 \end{pmatrix}, \tau_z^A = \begin{pmatrix} \mathbb{I}_2 & 0 \\ 0 & -\mathbb{I}_2 \end{pmatrix}. \quad (\text{B4})$$

BIBLIOGRAPHY

- [1] S. Mühlbauer et al., *Skyrmion Lattice in a Chiral Magnet*, *Science* **323** (2009) pg.:915-919
- [2] A. N. Bogdanov and D. A. Yablonskii, *Thermodynamically stable vortices in magnetic ordered crystals. The mixed state of magnets*, *Sov.Phys.JETP* **68**, 101-103 (1989).
- [3] A. N. Bogdanov and A. Hubert, *Thermodynamically stable magnetic vortex states in magnetic crystals*, *J.Magn.Magn.Mater.* **138** , 255-269 (1994).
- [4] U. K. Roessler, A. N. Bogdanov, and C. Pfleiderer, *Spontaneous Skyrmion Ground States in Magnetic Metals*, *Nature* **442** , pages 797–801 (2006).
- [5] A. N. Bogdanov and U. K. Rossler, *Chiral Symmetry breaking in magnetic thin films and multilayers*, *Phys.Rev.Lett.***87**, 037203 (2011).
- [6] C.Pfleiderer et al. , *Partial order in the non-Fermi-liquid phase of MnSi*, *Nature* **427**, 227-231 (2004).
- [7] S. Rohart and A. Thiaville, *Skyrmion Confinement in ultrathin film nanostructures in the presence of Dzyaloshinskii-Moriya Interaction*, *Phys.Rev.B* **88**, 184422 (2013).
- [8] B. Gobel, A. Mook, J. Henk and I. Mertig. *Antiferromagnetic skyrmion crystals: generation, topological Hall and topological spin Hall effect*, *Phys.Rev.B* **96**, 060406 (2017).
- [9] A. O. Leonov and M. Mostovoy , *Multiply periodic states and isolated skyrmions in an anisotropic frustrated magnet*, *Nature Communications* **6**, 8275 (2015).

- [10] L. Caretta et al. , *Fast current-driven domain walls and small skyrmions in a compensated ferrimagnet* , *Nature Nanotechnology* **13**, 1154–1160 (2018).
- [11] S. Seki, X. Z. Yu, S. Ishiwata¹ and Y. Tokura, *Observation of Skyrmions in a Multiferroic Material*, *Science* **Vol. 336** pp. 198-201 (2012).
- [12] A. Fert, N. Reyren, and V. Cros, *Advances in the Physics of Magnetic Skyrmions and Perspective for Technology* , *Nature Reviews Materials* **2**,, 17031 (2017).
- [13] N. Nagaosa and Y. Tokura, *Topological properties and dynamics of magnetic skyrmions* , *Nature Nanotechnology* **8**, pages 899-911 (2013).
- [14] R. Tomasello, E. Martinez, R. Zivieri, L. Torres, M. Carpentieri, and G. Finocchio. *A strategy for the design of skyrmion racetrack memories* , *Sci. Rep.* **4** , 6784 (2014).
- [15] T. H. R. Skyrme, *A Nonlinear field theory*, *Proc.Roy.Soc.Lond. A* **260** pg.:127-138 (1961).
- [16] C. Nash and S. Sen, *Topology and Geometry for Physicists*, Academic Press, 1983.
- [17] N. Manton and P. Sutcliffe, *Topological Solitons*, Cambridge University Press 2004.
- [18] A. A. Belavin and A. M. Polyakov, *Metastable states of two-dimensional isotropic ferromagnets* , *JETP Let.* **22**, issue 10,pg.245.
- [19] L. S. Leslie, A. Hansen, K. C. Wright, B. M. Deutsch, and N. P. Bigelow, *Creation and Detection of Skyrmions in a Bose-Einstein Condensate*, *Phys. Rev. Lett.* **103**, 250401 (2009).
- [20] J.Fukuda and S.Zumer, *Quasi Two-dimensional Skyrmion Lattices in a Chiral Nematic Liquid Crystal* , *Nature Communication* **2**, article no. 246 (2011).

- [21] S. L. Sondhi, A. Karlhede, S. A. Kivelson, and E. H. Rezayi, *Skyrmions and the crossover from the integer to fractional quantum Hall effect at small Zeeman energies*, *Phys. Rev. B* **47**, 16419 (1993).
- [22] C. Timm, S. M. Girvin, and H. A. Fertig, *Skyrmion lattice melting in the quantum Hall system*, *Phys. Rev. B* **58**, 10634 (1998).
- [23] L. D. Landau and E. M. Lifshitz, *Theory of the dispersion of magnetic permeability in ferromagnetic bodies*, *Phys. Z. Sowietunion* **8**, 153 (1935).
- [24] E. Fradkin, *Field Theories of Condensed Matter Physics*, Cambridge University Press, Second Edition (2013).
- [25] M. V. Berry, *Quantal phase factors accompanying adiabatic changes*, *Proc. R. Soc. Lond. A.* **392** (1984).
- [26] T. L. Gilbert, *Lagrangian formulation of the gyromagnetic equation of the magnetization field*, *Phys. Rev.* **100**, 1243 (1955).
- [27] T. Gilbert, *A phenomenological theory of damping in ferromagnetic materials*, *IEEE Transactions on Magnetics* **40**, 3443 (2004).
- [28] I. E. Dzyaloshinskii, *A thermodynamic theory of weak ferromagnetism of antiferromagnetics*, *J.Phys.Chem.Solids* **4**, 241 (1958).
- [29] T. Moriya, *New mechanism of anisotropic superexchange interaction*, *Phys.Rev.Lett.* **4**, 228 (1960).
- [30] P. Bak and M. H. Jensen, *Theory of helical magnetic structures and phase transitions in MnSi and FeGe*, *J. Phys. C: Solid St. Phys.* **13** (1980).
- [31] G. H. Derrick, *Comments on nonlinear wave equations as models for elementary particles*, *J. Math. Phys.***5**, 1252 (1964).

- [32] R. H. Hobart, *On instability of a class of unitary field models*, *Proc. Phys. Soc. Lond.* **82**, 201 (1963).
- [33] T. Schulz et al., *Emergent electrodynamics of skyrmions in a chiral magnet*, *Nature Physics*, **8** 301-304 (2012).
- [34] J. H. Han, J. Zang, Zhihua Yang, J. Park, and N. Nagaosa, *Skyrmion lattice in a two-dimensional chiral magnet*, *Phys. Rev. B* **82**, 094429 (2010).
- [35] X. Z. Yu, Y. Onose, N. Kanazawa, J. H. Park, J. H. Han, Y. Matsui, N. Nagaosa, and Y. Tokura, *Real Space Observation of a Two-dimensional Skyrmion Crystal*, *Nature* (London) **465**,901 (2010).
- [36] J. H. Han, *Skyrmions in Condensed Matter*, Springer Tracts in Modern Physics (2017).
- [37] M. Stone, *Magnus force on Skyrmions in ferromagnets and quantum Hall systems*, *Phys.Rev.B***53**, 16573 (1996).
- [38] C. Schutte and M. Garst. *Magnon-skyrmion scattering in chiral magnets*, *Phys. Rev. B* **90**, 094423 (2014).
- [39] N. Papanicolaou and T. N. Tomaras, *Dynamics of Magnetic Vortices*, *Nucl.Phys.B***360**, 425(1991).
- [40] A. A. Thiele, *Steady-State Motion of Magnetic Domains*, *Phys. Rev. Lett.* **30**, 230 (1973).
- [41] W. Nolting and A. Ramakanth, *Quantum Theory of Magnetism*, Springer-Verlag, 2009.
- [42] W. F. Brown, *Micromagnetics*, Wiley, New York (1963).

- [43] H.Ochoa and Y.Tserkovnyak, *Colloquium: Quantum Skyrmionics*, *Int. J. Mod. Phys. B* **33** no.21, 1930005 (2019).
- [44] J. R. Klauder, *Path integrals and stationary-phase approximations*, *Phys. Rev. D* **19** (8), 2349, (1979).
- [45] I. E. Dzyaloshinskii and G. E. Volovick, *Poisson brackets in condensed matter physics*, *Annals of Physics* **125** Pages 67-97 (1980).
- [46] P. J. Morrison, *Hamiltonian description of the ideal fluid*, *Rev. Mod. Phys.* **70**, 467 – (1998).
- [47] J. Wess and B. Zumino, *Consequences of anomalous Ward identities*, *Physics Letters B* **37**, 95- 97 (1971).
- [48] E. B. Sonin, *Magnus force in superfluids and superconductors* *Phys. Rev. B* **55**, 485 (1997).
- [49] A. Thiaville, S. Rohart, E. Jue, V. Cros, and A. Fert, *Dynamics of Dzyaloshinskii domain walls in ultrathin magnetic films*, *Europhysics Letters*, Volume 100, Number **5**, 2012.
- [50] M. A. Nielsen and I. L. Chuang, *Quantum Computation and Quantum Information*, Cambridge University Press; 10th Anniversary edition (2011).
- [51] R. Horodecki, P. Horodecki, M. Horodecki, and K. Horodecki, *Quantum entanglement*, *Rev. Mod. Phys.* **81** 865 (2009).
- [52] A. Einstein, B. Podolsky, and N. Rosen, *Can Quantum-Mechanical Description of Physical Reality Be Considered Complete?*, *Phys. Rev.* **47**, 777 (1935).
- [53] M. B. Plenio and S. Virmani. *An introduction to entanglement measures*, *Quant. Inf. Comput.* **7**:1-51 (2007).

- [54] M. W. AlMasri, *SU(4) description of bilayer skyrmion-antiskyrmion pairs*, to appear in Europhysics Letters 2020.
- [55] F. Jonietz et al. , *Spin Transfer Torques in MnSi at Ultralow Current Densities*, *Science* **330** , pp. 1648-1651 (2010).
- [56] J. Zang, M. Mostovoy, J. H. Han, and N. Nagaosa, *Dynamics of skyrmion crystal in metallic thin films* *Phys. Rev. Lett.* **107**, 136804 (2011).
- [57] W. Jiang et al. , *Direct Observation of the Skyrmion Hall Effect* *Nat.Phys.* **13** , 162 (2017).
- [58] R. Takashima, H. Ishizuka, and L. Balents, *Quantum skyrmions in two-dimensional chiral magnets*, *Phys. Rev. B* **94**, 134415 (2016).
- [59] F. Freimuth, R. Bamler, Y. Mokrousov, and A. Rosch, *Phase-Space Berry Phases in Chiral magnets: Dzyaloshinskii-Moriya interaction and the charge of skyrmions*, *Phys.Rev.B* **88**, 214409 (2013).
- [60] X. Zhang, Y. Zhou and M. Ezawa. *Magnetic bilayer-skyrmions without skyrmion Hall effect* , *Nat.Comm.* **7**, 10293 (2016).
- [61] W. Koshibae and N. Nagaosa. *Theory of skyrmions in bilayer systems* , *Sci.Rept.* **7**, 42645 (2017).
- [62] Y. M. Luo, C.Zhou, C. Won, and Y. Z. Wu, *Effect of Dzyaloshinskii-Moriya interaction on magnetic vortex* , *AIP Advances* **4**, 047136 (2014).
- [63] Z. F. Ezawa and G. Tsitsishvili, *SU(4) Skyrmions and Activation Energy Anomaly in Bilayer Quantum Hall Systems*, *Phys.Rev. B* **70** 125304 (2004).
- [64] K.Yang, S. Das Sarma, and A. H. MacDonald, *Collective Modes and Skyrmion Excitations in Graphene SU(4) Quantum Hall Ferromagnets*, *Phys. Rev. B* **74**, 075423 (2006).

- [65] B. Douçot, M. O. Goerbig, P. Lederer, and R. Moessner, *Entanglement Skyrmions in multicomponent quantum Hall systems*, *Phys.Rev.B* **78**, 195327 (2008).
- [66] J. M. Radcliffe, *Some properties of coherent spin states*, *J. Phys. A*, **7**, (1971).
- [67] D. Markham and V. Vedral, *Classicality of spin-coherent states via entanglement and distinguishability*, *Phys. Rev. A* **67** 042113 (2003).
- [68] L. Amico, R. Fazio, A. Osterloh, and V. Vedral, *Entanglement in Many-Body Systems*, *Rev.Mod.Phys.* **80**, 517-576 (2008).
- [69] I. Bengtsson and K. Życzkowski, *Geometry of Quantum States: An Introduction to Quantum Entanglement*, Cambridge University Press, Second Edition 2017.
- [70] J. P. Provost and G. Vallee, *Riemannian structure on manifolds of quantum states*, *Comm.Math.Phys.* **76**, 289-301 (1980).
- [71] Y. Lian, A. Rosch, and M. O. Goerbig, *SU(4) Skyrmions in the $\nu \pm 1$ Quantum Hall State of Graphene*, *Phys. Rev. Lett.* **117** 056806 (2016).
- [72] Y. Lian and M. O. Goerbig, *Spin-valley skyrmions in graphene at filling factor $\nu = -1$* , *Phys. Rev. B* **95**, 245428 (2017).
- [73] D. C. Brody and L. P. Hughston, *Geometric Quantum Mechanics*, *J.Geom.Phys.* **38** 19-53 (2001).
- [74] M. Gell-Mann and Y. Ne'eman, *The Eight-Fold Way*, Benjamin, New York 1964.